

Mass-independent analysis of the stable isotopologues of gas-phase titanium monoxide – TiO

Alexander A. Breier^{a,*}, Björn Waßmuth^a, Guido W. Fuchs^a, Jürgen Gauss^b, Thomas F. Giesen^a

^aLaboratory for Astrophysics, Institute of Physics, University of Kassel, 34132 Kassel, Germany

^bInstitut für Physikalische Chemie, Universität Mainz, 55099 Mainz, Germany

Abstract

More than 130 pure rotational transitions of ^{46}TiO , ^{47}TiO , ^{48}TiO , ^{49}TiO , ^{50}TiO , and $^{48}\text{Ti}^{18}\text{O}$ are recorded using a high-resolution mm-wave supersonic jet spectrometer in combination with a laser ablation source. For the first time a mass-independent Dunham-like analysis is performed encompassing rare titanium monoxide isotopologues, and are compared to results from high-accuracy quantum-chemical calculations. The obtained parametrization reveals for titanium monoxide effects due to deviations from the Born-Oppenheimer approximation. Additionally, the dominant titanium properties enable an insight into the electronic structure of TiO by analyzing its hyperfine interactions. Further, based on the mass-independent analysis, the frequency positions of the pure rotational transitions of the short lived rare isotopologue ^{44}TiO are predicted with high accuracy, i.e., on a sub-MHz uncertainty level. This allows for dedicated radio-astronomical searches of this species in core-collapse environments of supernovae.

Keywords: TiO, titanium monoxide, isotopologues, mass-independent analysis, supersonic jet expansion, mm-wave, electronic structure, FACM

1. Introduction

Since the beginning of the 20th's century TiO (titanium monoxide) belongs to one of the best studied diatomic molecules of astrophysical relevance [1, 2]. The molecule is routinely used to characterize circumstellar environments [3, 4, 5] and to classify stars within the MK spectral classification scheme [6, 7, 8]. Recently, TiO has been also observed in hot exoplanet atmospheres [9, 10, 11, 12].

The rare and non-stable titanium isotope ^{44}Ti is of general interest for the understanding of processes that take place in core-collapse supernovae, where it is thought to be synthesized in significant quantities [13, 14]. In principle, the γ -ray emission from the decay of ^{44}Ti nuclei can be used as a tool for the search of remnants of recent supernovae (less than approx 1,000 years old) [15]. However, an unambiguous assignment of the X- and γ -ray emission of ^{44}Ti to specific sources has been so far only possible in the case of the

*Corresponding author

Email address: a.breier@physik.uni-kassel.de (Alexander A. Breier)

supernovae remnant (SNR) Cassiopeia A using the IBIS/ISGRI instrument on board of the INTEGRAL satellite [16, 17] and for SN 1987A using the NuSTAR space observatory [18].

An alternative approach to identify the rare isotope in these environments could be the detection of the diatomic molecule ^{44}TiO at radio wavelengths where modern large scale facilities, like ALMA (Atacama Large Millimeter/submillimeter Array), allow for high spatial resolution and high sensitivity. The short lifetime of ^{44}Ti of 58.9 ± 0.3 a [19] hinders an easy laboratory approach to the accurate determination of the rotational transitions of this molecule. However, mass-independent studies of titanium monoxides can be used to accurately predict the line positions.

Observations of ^{44}TiO and other more easily to detect stable isotopologues could result in valuable information about the fractional abundance of the titanium isotopes as result of core-collapse dynamics. In this work a mass-independent study has been performed using the Dunham approach [20, 21] which besides its astronomical interest concerning the ^{44}TiO is also of fundamental spectroscopic interest. The use of Dunham coefficients is a powerful tool that allows to obtain a comprehensive picture of diatomic molecules independent of the individual isotope composition. It includes aspects of the potential anharmonicity, the interaction between vibrational and electronic motion and effects of the Born-Oppenheimer breakdown and thus combines many aspects of molecular motion which results in high-accuracy parameters. In addition, the structure of TiO can be determined purely from experimental data by this method. For this to work many data from previous experiments is combined starting with publications from the late 1920, e.g., the first assigned electronic TiO α system ($C^3\Delta - X^3\Delta$) [22], until recent work by Lincowski *et al.* [23] about rotational transitions of several titanium isotopologues. There exist five stable Ti isotopes, namely $^{46-50}\text{Ti}$ and three oxygen isotopes $^{16-18}\text{O}$. In this work six out of the fifteen possible combinations have been investigated ($^{46-50}\text{Ti}^{16}\text{O}$ and $^{48}\text{Ti}^{18}\text{O}$).

2. Titanium monoxide

A rich literature is available about the rovibronic energy levels of the main isotopologue $^{48}\text{Ti}^{16}\text{O}$ which has been summarized by McKemmish *et al.* [24]. In the here presented work the laser-induced fluorescence (LIF) studies of the γ' system ($B^3\Pi - X^3\Delta$) [25] and γ ($A^3\Phi - X^3\Delta$) [26] are of particular interest.

The ^{47}TiO isotopologue was observed by Fletcher *et al.* [27] using the high-resolution molecular beam LIF spectra from the $\gamma'(0,0)$ band and the ground-state hyperfine parameters of ^{47}Ti ($I=5/2$) were determined by using combination difference analysis. In the work of Barnes *et al.* [28] all isotopologues were observed in the $\gamma(0,0)$ system by their LIF signals from a double-resonance experiment of rotationally jet-cooled TiO. More recently the $\gamma'(1,0)$ band of ^{46}TiO was investigated by analysis of the LIF spectra by Amiot *et al.* [29]. In the same year Kobayashi *et al.* [30] observed all stable isotopologues by measuring the ($E^3\Pi - X^3\Delta$) transitions.

For the main isotopologue ^{48}TiO purely high-resolution rotational data of the ground state were investigated by Namiki *et al.* [31] and Kania *et al.* [32]. Recently, Lincowski *et al.* [23] presented rotational measurements of all stable titanium isotopologues.

From previous works [25, 27] it can be concluded that the electronic ground state $X^3\Delta$ is well represented by a $\dots(8\sigma)^2(3\pi)^4(9\sigma)^1(1\delta)^1$ electron configuration with two unpaired electrons occupying the 9σ and 1δ orbital. The $(9\sigma)^1$ molecular orbital (MO) originates mainly from the atomic Ti $4s$ and the MO $(1\delta)^1$ comes from a pure atomic Ti $3d$ orbital. This makes TiO the simplest molecule with a $3d$ orbital used in a molecular bonding [33]. Furthermore, the two unpaired electrons are predicted to strongly polarize the molecule [27, 34] resulting in a $X^3\Delta$ state as lowest electronic configuration. This leads to a coupling of the electronic ($\Lambda = 2$) and the spin ($\Sigma = 1$) angular momentum according to Hund's case (*a*) resulting in three energetically well separated sub states $^3\Delta_1$, $^3\Delta_2$ and $^3\Delta_3$ (adapting the usual nomenclature $^{2\Sigma+1}\Lambda_\Omega$ with $\Omega = \Lambda - \Sigma, \dots, \Lambda + \Sigma$), see Fig. 3. The analysis of optical Stark spectra shows a permanent electrical dipole moment of 3.34(1) D for the ground state $X^3\Delta_1$ [35].

3. Experiment

High-resolution sub-mm-wavelength absorption spectra of 132 TiO rotational transitions in the ground state ($X^3\Delta$) have been recorded using the Supersonic Jet Spectrometer for Terahertz Applications (Su-JeSTA). The experimental setup has been described in Ref. [36].

In brief, a 1064 nm intense Q-switched Nd:YAG laser beam at 30 Hz repetition rate is focused on a solid titanium rod (99,6% purity, Goodfellow). The ablated material is seeded in either a pulsed gas flow of a 5% N_2O or a 1.25% O_2 mixture in helium. For measurements on the Ti^{18}O isotopologue an admixture of $^{18}\text{O}_2$ (Campro Scientific GmbH, 97 atom %) is used with a mixing ratio $^{18}\text{O}_2:^{16}\text{O}_2$ of 1:5, which allows to control the stability of molecular production by checking to the signal of the most abundant TiO isotopologue. The gas at room temperature has a 2 bar stagnation pressure at the injecting valve but before reaching the titanium rod, it undergoes adiabatic pre-cooling to below 100 K.

During a few μsec the ablated titanium can chemically react with the gas mixture in a $\approx 100 \text{ mm}^3$ large reaction channel at a few hundred mbar pressure before adiabatically expanding into a vacuum chamber where it can be observed as supersonic jet (see [37] for more details on the ablation source). Fig. 1 shows a supersonic jet expansion with well pronounced shock fronts. To enhance the contrast of the photograph we used argon instead of helium which emits intense blue light from electronically excited states. The TiO molecules seeded in the adiabatically cooled helium jet interact with a submm-wavelength probe beam 20 mm down-stream from the nozzle exit, where they have a rotational temperature of a few tens Kelvin.

A multi-pass optics (12 paths Herriott type) perpendicular to the jet propagation is used to enhance the absorption. Radiation between 250 to 385 GHz is produced by a cw-operating cascaded multiplier chain

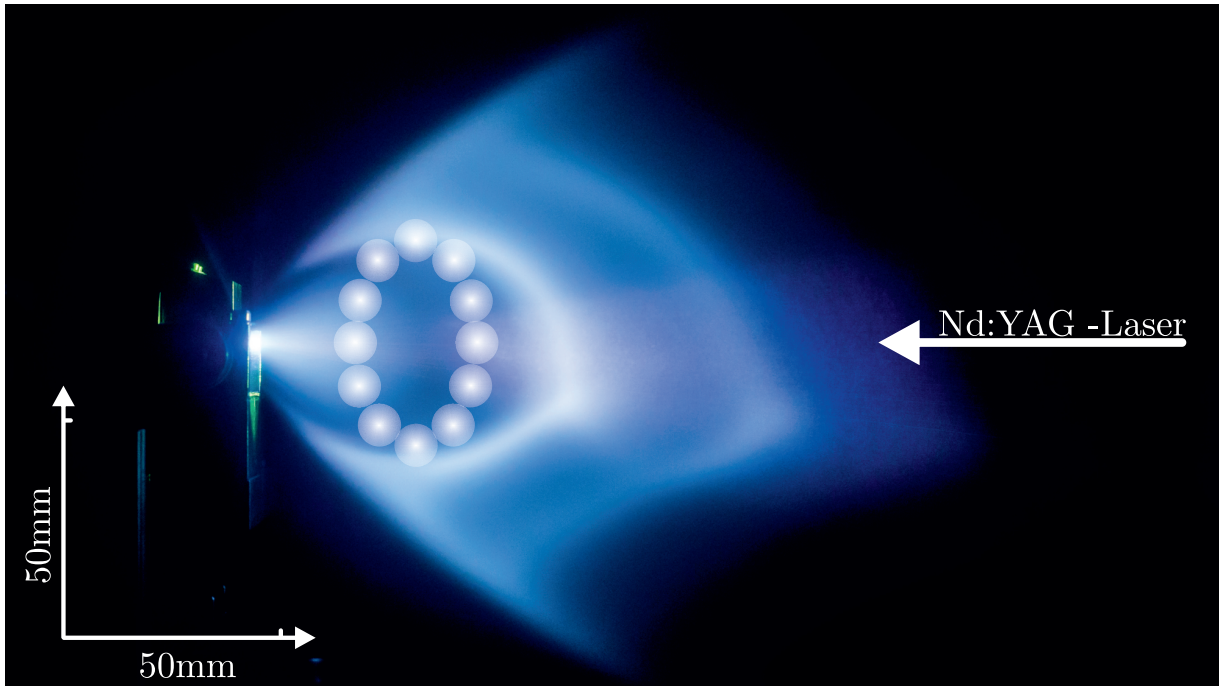


Fig. 1: Photograph of a supersonic jet (Exposure time: 2.9s, f5.6, ISO 3200) superimposed with a sketch of a multi-reflection submm-wavelength beam (300 GHz). The jet contains titanium vapor from a laser ablation, seeded in argon buffer gas (2 bar).

(AMC-9 + triple stage from Virginia Diodes, VDI) where the 9 to 14 GHz output signal of a tunable synthesizer (VDI) is amplified and frequency multiplied by a factor of 27. The signal is detected by a liquid-He cooled InSb hot-electron bolometer (QMC instruments) and data is recorded during a $100 \mu\text{s}$ time window. A low-noise amplifier and band-pass filter (SR560, Scientific Instruments) is used to reduce the low frequency noise of the signal before storing the time-dependent signal on a computer. A 0.1 MHz step-scan modus is used to scan over spectral ranges of typically 40-50 MHz, to cover individual rotational TiO lines, and their hyperfine components. To increase the signal-to-noise ratio the signal at each frequency position is averaged over eight laser shots. The accuracy of the measured line center positions is 10 kHz with typical line widths (FWHM) of 0.6 MHz.

4. Measurements and Data Reduction

We measured 132 ground-state rotational absorption transitions of TiO in natural abundance [38, 39] and assigned 14 lines to the main isotopologue $^{48}\text{TiO}^1$ (73.72%) and 13 lines to each of the less abundant

¹If not otherwise stated O refers to the ^{16}O isotope.

isotopologues ^{46}TiO (8.25%) and ^{50}TiO (5.18%) (see Tab. 8). Although, the rotational temperature in the jet is low, we were able to measure all spin-orbit components ($\Omega = 1, 2,$ and 3) with a signal-to-noise ratio of better than 5. Species of the odd numbered nuclei, ^{47}Ti and ^{49}Ti , exhibit prominent hyperfine spectra due to nuclear spins of $I(^{47}\text{Ti})=5/2$ and $I(^{49}\text{Ti}) = 7/2$, respectively. We measured 47 ^{47}TiO (7.44%) transitions encompassing five lines of the $^3\Delta_1$ spin-orbit component and three $^3\Delta_2$ lines each with six hyperfine components (except one weak line). For ^{49}TiO (5.41%) 40 transitions of the $^3\Delta_1$ component were recorded encompassing five rotational transitions with eight hyperfine splittings each (see Tab. 10). Furthermore, we recorded five rotational transitions of the $^3\Delta_1$ state of $^{48}\text{Ti}^{18}\text{O}$ (see Tab.9). For the main isotopologue ^{48}TiO ($X^3\Delta_2$) two rotational transitions in their first vibrationally excited state ($\nu=1$) have been observed. In addition, we observed eight not yet measured titanium dioxide (TiO_2) lines, listed in Tab. 13.

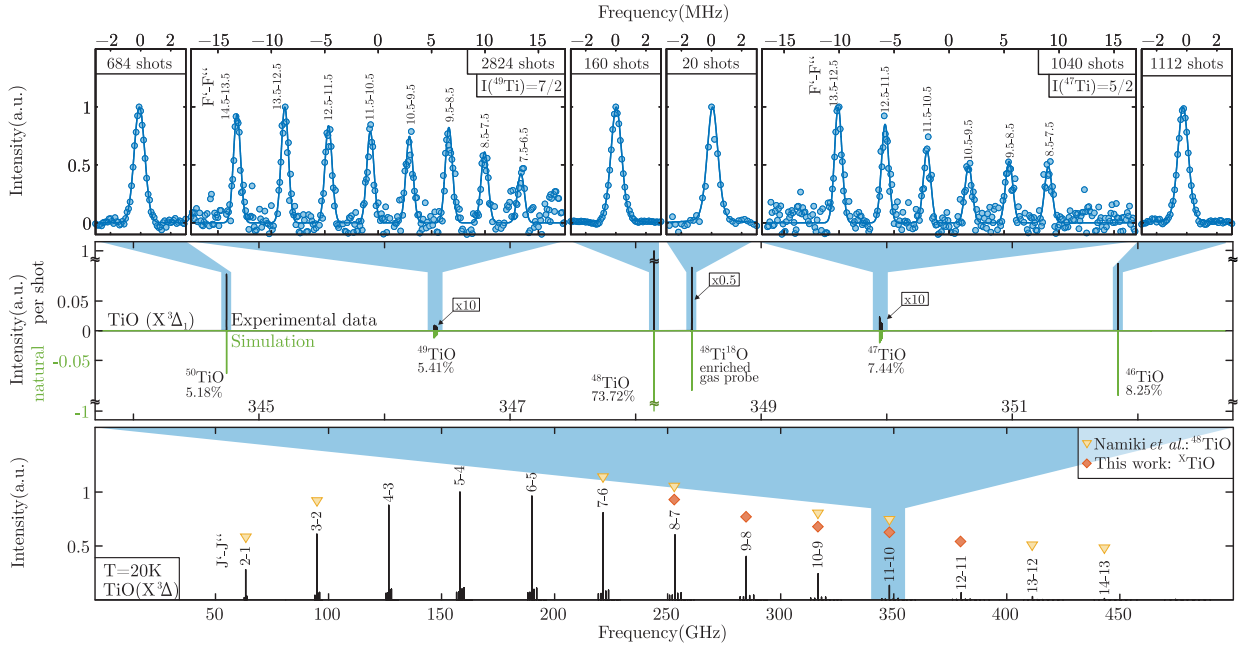


Fig. 2: The bottom frame shows simulated stick spectra of titanium monoxide in the rotational ground state, $X^3\Delta$, at a temperature of 20 K and frequencies up to 500 GHz. Triangles mark the previously measured rotational transitions of the main isotopologue ^{48}TiO by Namiki *et al.* [31]. Rotational transitions measured in this work are labeled with diamonds. The middle frame gives a closer look at the rotational transitions of the TiO isotopologues of $J''=10$ in the frequency range of 344–352 GHz with calculated line strength (green) and experimental values for the intensity per laser shot (black) with respect to ^{48}TiO . The upper frames show examples of measured line profiles (dots) and fitted Voigt profiles (blue solid line).

To each of the measured transitions a Voigt profile was fitted and line-center frequencies were determined with 1σ -uncertainties of less than 0.1 MHz. The here presented molecular parameters of TiO were determined by a combined analysis of high-resolution data including electronic transitions in the optical range

as well as rotational transitions in the GHz region. From the electronic spectra of ^{48}TiO we included nearly 8000 transitions of the ($A^3\Phi - X^3\Delta$) system observed by Ram *et al.* [26] and roughly 1300 transitions of the ($B^3\Pi - X^3\Delta$) system investigated by Amiot *et al.* [25]. The measured data set were kindly provided by C. Amiot upon request. In the GHz range, the ^{48}TiO data set from Namiki *et al.* [31] and recently published data of titanium isotopologues ($^{46,47,49,50}\text{TiO}$) from Lincowski *et al.* [23] are taken into account in addition to our high-resolution data from the present work. To combine the experimental datasets from different apparatus, a two-step fitting routine is used. In the first step the datasets are included with their reported frequency uncertainties as weighting factor [40]. Subsequently, the sub-datasets are evaluated with respect to their weighted standard deviation value. This value was used to scale the weighting factor of the final fitting step. The literature data set errors are 1.021 (Amiot *et al.* [25]), 2.468 (Namiki *et al.* [31]), 1.234 (Ram *et al.* [26]) and 1.209, 2.077, 2.478, 1.484 (^{46}TiO , ^{47}TiO , ^{49}TiO , ^{50}TiO , Lincowski *et al.* [23]). The program PGOPHER [41] is used to evaluate the N^2 Hamiltonian representation for all isotopologues. Beside the pure rotational parameters (B_ν , D_ν , and H_ν) for the ro-vibrational parametrization of the $X^3\Delta$ and $A^3\Phi$ state further parameters have to be considered such as the state origin (T_ν), the spin-orbit coupling parameters (A_ν , A_{D_ν}), the spin-rotation coupling parameter (γ), and the spin-spin coupling parameter (λ_ν , λ_{D_ν}). In addition, for the stable isotopes with a non-vanishing nuclear spin moment the hyperfine coupling parameters (a_ν , b_ν , c_ν , $b_{D,\nu}$, $c_{D,\nu}$, $eQq_{0,\nu}$) have to be considered. It is known [23] that the hyperfine spin-orbit interaction for the $^3\Delta_2$ state is perturbed by the $a^1\Delta$ state, which is represented in the fit by the parameter Δa . In the case of the $B^3\Pi$ state the λ -doubling parameters (o , o_D , o_H , p , p_D , q , q_D) need to be taken into account. Considering the well-known mass dependencies for diatomic molecules shown by Dunham [20] and in related work by Ross and Watson [42, 43, 44], the size of the parameter space is reduced from nearly 200 individual molecular parameters to 69 mass-independent parameters. The following general equation was used in the Dunham-type multi-isotopologue analysis to constrain the molecular parameters (see also Breier *et al.* [45])

$$X_{\nu,\alpha} = \sum_k \eta \cdot \mu_\alpha^{-\frac{2l+k}{2}} \cdot \hat{O}_{k,l} \cdot \left(1 + \sum_{i=A,B} \frac{m_e}{M_\alpha^i} \Delta_{\hat{O}_{k,l}}^i \right)_{BO} \cdot \left(\nu + \frac{1}{2} \right)^k. \quad (1)$$

The molecular parameter $X_{\nu,\alpha}$ of isotopologue α in its vibrational state ν is represented by a sum over Dunham-like expansion terms. Here $X_{\nu,\alpha}$ is one of the parameters $T_{\nu,\alpha}$, $B_{\nu,\alpha}$, $D_{\nu,\alpha}$, ..., given in Tab. 1. The index k denotes the ro-vibrational coupling order and l stands for the molecular parameter expansion order (e.g. $l=0 \rightarrow U_{k,0} \rightarrow T_\nu$, and $l=1 \rightarrow U_{k,1} \rightarrow B_\nu$). Each term in Eq. 1 consists of five factors, the first being the effective proportional factor η . For most parameters, this scaling factor is simply one, but for the hyperfine parameters a , b , c , and c_I this factor is equal to the nuclear g factor (g_N) and for the case of the eQq_0 parameter it is equal to the nuclear quadrupole moment Q , see [46, 47] for more details. For ^{47}Ti and

^{49}Ti , the used g_n factors are 0.315392(4) and 0.315477(3) [48, 49], respectively, and are determined by their nuclear magnetic dipole moment. Pyykkö [50] reviewed the values for the nuclear quadrupole moments as $Q(^{47}\text{Ti})=0.302(10)$ barn and $Q(^{49}\text{Ti})=0.247(11)$ barn. The second factor from Eq. 1 represents the reduced mass-scaling factor μ_α of an isotopologue α of the diatomic molecule AB . Thereon the isotopic invariant factor $\hat{O}_{k,l}$ follows, which is a placeholder for the actual molecular parameter to be fitted, e.g., in the case of $X_{\nu,\alpha}$ being $T_{\nu,\alpha}$ the invariant factor $\hat{O}_{k,l}$ is $U_{k,0}$, see Tab. 1. The subindexes of \hat{O}_{kl} are mostly identical to former publications despite parameters reflecting the spin-rotational contributions like, γ or c_I . These are shifted in the l -index following directly their reduced mass-dependency of μ^{-1} [51]. The fourth factor (term in parentheses) handles the Born-Oppenheimer breakdown (BO) which is different for each isotopic invariant parameter. The sum index i refers to the atoms A and B of the diatomic molecule, e.g., A=Ti and B=O. Further, m_e is the electron mass, M^A is the mass of atom A and $\Delta_{\hat{O}_{k,l}}^A$ is the to-be-fitted BO coefficient of atom A. The same procedure applies to atom B. Our dataset leads to the BO terms of the first-order rotational expansion term U_{01} and the centrifugal-distortion term of the spin-orbit coupling A_{01} with respect to titanium. The last factor of Eq.1 describes the ro-vibrational coupling of the expansion terms. As an example $X_{\nu,\alpha}$ for $\nu=0$, $\alpha=^{48}\text{Ti}^{16}\text{O}$ and $l=1$, i.e. $B_{0,48\text{Ti}^{16}\text{O}}$, is

$$B_0 = \mu^{-1}U_{01} \cdot \left(1 + \frac{m_e}{M^{Ti}} \cdot \Delta_{U_{01}}^{Ti} + \frac{m_e}{M^O} \cdot \Delta_{U_{01}}^O\right)_{BO} + \quad (2a)$$

$$\mu^{-1.5}U_{11} \cdot \left(0 + \frac{1}{2}\right) + \mu^{-2}U_{21} \cdot \left(0 + \frac{1}{2}\right)^2 + \mu^{-2.5}U_{31} \cdot \left(0 + \frac{1}{2}\right)^3 \quad (2b)$$

$$\equiv Y_{01} + Y_{11} \cdot \left(0 + \frac{1}{2}\right) + Y_{21} \cdot \left(0 + \frac{1}{2}\right)^2 + Y_{31} \cdot \left(0 + \frac{1}{2}\right)^3 \quad (2c)$$

with

$$\mu = \frac{M^{Ti}M^O}{M^{Ti} + M^O} \quad (\text{see Tab. 2}).$$

Note that not only the mass-independent U_{ij} coefficients are given here but also the mass-dependent Dunham coefficients Y_{ij} are shown in Eq. 2c and they will be discussed in Sec. 6.2. The BO contributions in the terms 2b are set to zero.

In our analysis we have used mass units that have been compiled and referenced in the latest evaluation of atomic masses, AME2016 [52]. One should notice, that for a single-isotope fit, the effects on A_D and γ are not distinguishable in terms of energy in a $^3\Delta$ electronic state. Performing an isotopic invariant fitting procedure allows to distinguish between these contributions [46]. Therefore, two different fitting procedures were used: *Fit A* is without the contribution of the spin-rotational parameter γ while *Fit B* is taking the contribution of γ into account (see Tab.11). For the first time a spin-rotational value for TiO is determined as 233.8(17) MHz. However, in the following discussion section, we stick to the mass-independent parameter set of *Fit A*, which resulted in a smaller value of the weighted error. Furthermore, comparing our results to former published data [26, 23] is straight forward when using *Fit A*. The results of our PGOPHER simulations

Tab. 1: Translation of the effective molecular parameters $X_{\nu,\alpha}$ to the mass-independent Dunham-like parameters $\hat{O}_{k,l}$ and the effective proportional factor η as given in Eq. 1.

| $X_{\nu,\alpha}$ | $\hat{O}_{k,l}$ | η | $X_{\nu,\alpha}$ | $\hat{O}_{k,l}$ | η |
|------------------------|-----------------|--------|----------------------------|------------------|------------------|
| $T_{\nu,\alpha}$ | $U_{k,0}$ | 1 | $\lambda_{D_{\nu,\alpha}}$ | $\lambda_{k,1}$ | 1 |
| $B_{\nu,\alpha}$ | $U_{k,1}$ | 1 | $a_{\nu,\alpha}$ | $a_{k,0}$ | \mathfrak{g}_N |
| $D_{\nu,\alpha}$ | $U_{k,2}$ | 1 | $\Delta a_{\nu,\alpha}$ | $\Delta a_{k,0}$ | \mathfrak{g}_N |
| $H_{\nu,\alpha}$ | $U_{k,3}$ | 1 | $b_{\nu,\alpha}$ | $b_{k,0}$ | \mathfrak{g}_N |
| $\gamma_{\nu,\alpha}$ | $\gamma_{k,1}$ | 1 | $c_{\nu,\alpha}$ | $b_{k,0}$ | \mathfrak{g}_N |
| $A_{\nu,\alpha}$ | $A_{k,0}$ | 1 | $b_{D_{\nu,\alpha}}$ | $b_{k,1}$ | \mathfrak{g}_N |
| $A_{D_{\nu,\alpha}}$ | $A_{k,1}$ | 1 | $c_{D_{\nu,\alpha}}$ | $c_{k,1}$ | \mathfrak{g}_N |
| $\lambda_{\nu,\alpha}$ | $\lambda_{k,0}$ | 1 | $eQq_{0,\nu,\alpha}$ | $eQq_{0,k,0}$ | Q |

are available as supplementary material.

5. Quantum-chemical calculations

High-accuracy quantum-chemical calculations were carried out to support the experimental investigations. All of them were performed at the coupled-cluster (CC) level [53] using large correlation-consistent basis sets [54]. To be more specific, the equilibrium distance of TiO was determined using a composite scheme together with basis-set extrapolation, as described in Refs. [55, 56]. The extrapolation at the Hartree-Fock level [57] was based on results cc-pwCVXZ (X=T,Q, and 5) basis sets [58, 59], while the extrapolation at the CCSD(T) level [60, 61] has been carried out using the cc-pwCQZ and cc-pwC5Z sets. Additional corrections account for the difference of CCSD(T) to the full CC singles, doubles, triples (CCSDT) treatment [62] (as computed using a cc-pVTZ basis) and for the effect of quadruple excitations at the CC singles, doubles, triples, quadruples (CCSDTQ) level [63] (as computed at the cc-pVDZ level). Furthermore, scalar-relativistic corrections were considered at the spin-free X2C-1e level [64, 65, 66, 67]; these calculations were carried out with an uncontracted ANO-RCC basis set [68, 69].

Based on previous experience [56], the overall accuracy of the computed TiO bond distance should be in the range of about 0.002 Å. This accuracy is for most spectroscopic purposes sufficient, but it does not match the accuracy provided by a Dunham analysis. Thus, we refrain from a detailed computational study of the other spectroscopic parameters, though in principle possible, and in the following only provide computational data for the Born-Oppenheimer breakdown or correction parameters. These parameters were computed as outlined in Refs. [70, 71]. The required rotational g-tensor [72] were determined at the frozen-core CCSD(T)

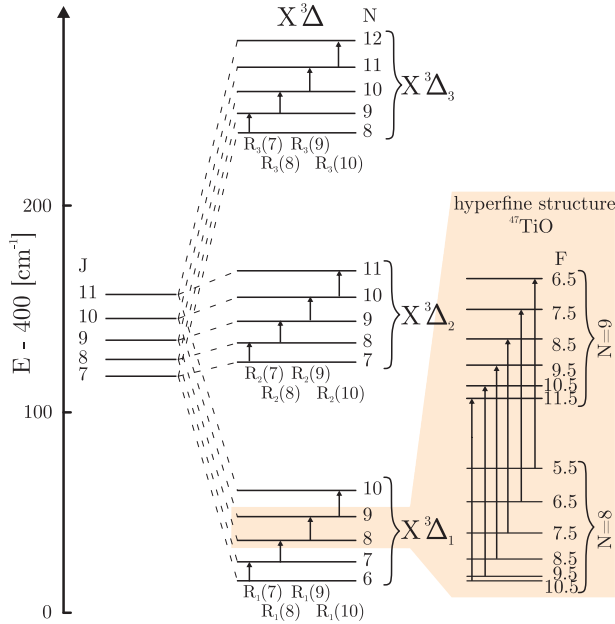


Fig. 3: Fine and hyperfine structure of ($X^3\Delta$) TiO. The spin-orbit components are separated by 100 cm^{-1} . For ^{47}TiO the hyperfine splitting of the $X^3\Delta_1$, $N = 9 \leftarrow N = 8$, and $\Delta F = +1$ transitions are depicted.

level using the aug-cc-pVTZ basis [73], while the adiabatic correction to the bond distance is obtained via the computation of the diagonal Born-Oppenheimer correction [74] (performed at the CC singles, doubles (CCSD) level using the cc-pwCVTZ basis [54, 59]). The usually rather small Dunham correction was not considered in the present work.

All calculations were carried out using the CFOUR program package [75].

6. Discussion and Conclusion

In this section the discussion is based on experimental measurements and on quantum-chemical calculations. In Sec. 6.1 we apply the mass-independent Dunham-like parametrization to TiO. Section 6.2 is concerned with the analysis of the TiO molecular structure dominated by the mass-independent rotational parameter U_{01} (see Eq. 2) and the corresponding BO terms. The topic of Sec. 6.3 is the electronic structure of the TiO molecule. Based on the free atom comparison method, the molecular bonding is investigated by analysis of the molecular hyperfine parameters of the odd TiO isotopologues.

6.1. Mass-independent Dunham-like parameterization

High-resolution measurements of stable isotopologues allow the determination of ground-state molecular parameters to high precision, see Tab. 2. The value of the first-order expansion term of the rotational constant for the main isotopologue (i.e., the U_{01} containing term of B_0 see Eq. 2a) is determined

Tab. 2: Comparison of mass-depending molecular parameters and bond lengths for the various TiO isotopologues.

| | $\mu_\alpha(\text{u})$ | $\tilde{A}_{01}(10^5\text{cm}^{-1})$ | $Y_{01}(\text{cm}^{-1})$ | $r_e(\text{\AA})$ |
|-------------------------------|------------------------|--------------------------------------|--------------------------|-------------------|
| $^{46}\text{Ti}^{16}\text{O}$ | 11.865012325(12) | -2.6763(27) | 0.541147722(47) | 1.620340280(71) |
| $^{47}\text{Ti}^{16}\text{O}$ | 11.930564845(8) | -2.6370(27) | 0.538175512(46) | 1.620338581(70) |
| $^{48}\text{Ti}^{16}\text{O}$ | 11.993884458(8) | -2.5997(26) | 0.535335382(46) | 1.620336957(70) |
| $^{49}\text{Ti}^{16}\text{O}$ | 12.055488302(7) | -2.5640(26) | 0.532600833(46) | 1.620335394(70) |
| $^{50}\text{Ti}^{16}\text{O}$ | 12.115047227(8) | -2.5301(26) | 0.529983487(46) | 1.620333898(70) |
| $^{48}\text{Ti}^{18}\text{O}$ | 13.086589627(9) | -4.0629(130) | 0.490647357(47) | 1.620318041(77) |

as $0.535335379(46)\text{cm}^{-1}$ and agrees well with the value observed by Ram *et al.* of $0.53533536(16)\text{cm}^{-1}$ (see p_0 value of B_ν in Tab. 7 of [26]). Thanks to the available large data set for the main isotopologue, and applying mass-invariant scaling, the same high accuracy can be reached for the parameters of the rare isotopologues. The consistency of the determined mass-invariant parameters can be checked by applying the so-called Kratzer [76] and Pekeris [77] relation: $U_{02} = 4U_{01}^3/U_{10}^2$, which results in $8.676010(16)\cdot 10^{-5}\text{cm}^{-1}\text{u}^2$. The direct determination of U_{02} using Eq. 1 yields $8.67181(37)\cdot 10^{-5}\text{cm}^{-1}\text{u}^2$ and thus is in good agreement with the above value given that the BO correction terms are not considered in this approach. Furthermore, we can easily extract the dissociation-energy value of $6.92053(56)\text{eV}$ for the ground state from the relation $\mathcal{D}_e = \frac{\omega_e^2}{4\omega_e X_e} \hat{=} \frac{U_{10}^2}{4U_{20}}$ ([78]). Despite the restriction to a simple Morse potential [79], the result is in very good agreement with the values derived from crossed-beam studies by Naulin *et al.* [80] with $\mathcal{D}_e = 6.87_{-0.05}^{+0.07}\text{eV}$ and as well from a potential analysis of the electronic ground-state performed by Reddy *et al.* [81] resulting in $6.94(16)\text{eV}$.

Tab. 3: Comparison of the different r_e distances for TiO

| | bond length (\AA) | (Comment) |
|--------------------------|------------------------------|------------------------|
| r_e^{48} | 1.62033709(25) | Ram <i>et al.</i> [26] |
| r_e^{48} | 1.620336957(70) | This work |
| \bar{r}_e | 1.62033386(527) | This work |
| r_e^{BO} | 1.62009060(31) | This work |
| $r_{e,theo}^{\text{BO}}$ | 1.6189 | This work |

6.2. Molecular structure of ($X^3\Delta$) TiO

From measurements of six TiO isotopologues the bond length of TiO can be obtained via the moment of inertia $I_e = \mu r_e^2$ and the related rotational constant B_e [78]. In the literature B_e is derived from the mass-dependent Dunham coefficient Y_{01} , provided that $Y_{01} \approx B_e$ is a good approximation [20]. The r_e bond length of six TiO isotopologues are given in Tab. 2 and they significantly scatter about a mean value \bar{r}_e of 1.62033386(527) Å. For $^{48}\text{Ti}^{16}\text{O}$ Ram *et al.* published a bond length $r_e^{48} = 1.62033709(25)$ Å which is in excellent agreement with the value derived from the present study. The derivation of isotopic-specific bond lengths are clear indications for deviations from the Born-Oppenheimer approximation. A mass-independent approach which includes the Born-Oppenheimer breakdown (BO) coefficients (see Eq. 2a) is given by

$$B_e = U_{01} \cdot \mu^{-1} \quad \text{and} \quad r_e^{\text{BO}} = U_{01}^{-1/2} \cdot \left(\frac{\hbar}{4\pi} \right)^{1/2}, \quad (3)$$

where r_e^{BO} is the mass-independent BO corrected bond length, which is given as $r_e^{\text{BO}} = 4.1058043277(10)U_{01}^{-1/2}$ with U_{01} given in units of atomic mass units u and wavenumbers cm^{-1} , and the distance given in Å.

The derived bond length is 1.62009060(31) Å and shown in Tab. 3. The BO distance is significantly smaller (by about 0.00024 Å) than all the mass-dependent values, as is usually the case.

This value should be also compared to the best theoretical estimate for the TiO bond distance of 1.6189 Å as obtained using a composite approach with corrections for scalar-relativistic effects. The theoretical value thus is too short in comparison with experimentally derived distance, but the discrepancy is within the usual error margin of high-accuracy state-of-the-art predictions [82]. It is also interesting to note that without consideration of scalar-relativistic effects an even shorter distance is obtained, namely 1.6176 Å, scalar-relativistic effects thus amount to about 0.0012 Å and are not negligible. Furthermore, the importance of higher excitations should be noted, as pure CCSD(T) computations (extrapolated to the basis-set limit) yield 1.6099 Å, i.e., a value which is about 0.008 Å too short compared to the best non-relativistic value. Corrections for a full triple excitations treatment amount to 0.004 Å, the corrections for quadruple excitations are of the same order of magnitude.

Titanium is a group 4 element in the periodic table, such as zirconium (Zr) and hafnium (Hf). By comparing the r_e value of ^{48}TiO to those of the most abundant isotopologues of ZrO and HfO (see Tab. 4) it is seen that the bond length increases with the row number. For all three oxides, the determined mass-independent r_e^{BO} values are smaller than the respective mass-dependent r_e values, which is a consequence of the electron-nucleus interaction that is considered by the BO breakdown term. Note that the difference $|r_e - r_e^{\text{BO}}|$ is of same order for TiO, ZrO, and HfO.

Looking at monoxides of the neighboring elements in the periodic table. i.e., scandium monoxide (ScO) and vanadium monoxide (VO), it is noted that the bond lengths decrease with increasing atomic number, which can be attributed to the influence of δ -orbital [34].

Tab. 4: Comparison of dipole moment, r_e and mass independent Born-Oppenheimer correction term for $^{48}\text{Ti}^{16}\text{O}$ and related main isotopologues of transition metal diatomic molecules.

| Molecule (AB) | $\mu(\text{D})$ | $r_e(\text{\AA})$ | $r_e^{\text{BO}}(\text{\AA})$ | Δ_{U01}^{A} | Δ_{U01}^{B} |
|----------------------------------------|-----------------|-------------------|-------------------------------|---------------------------|---------------------------|
| TiO($X^3\Delta$) ^a | 3.34(1) | 1.62033696(7) | 1.62009060(31) | -8.253(24) | -6.112(8) |
| ZrO($X^1\Sigma^+$) ^b | 2.551(11) | 1.71195242(73) | 1.711174527(74) | -4.872(39) | -6.189(3) |
| HfO($X^1\Sigma^+$) ^c | 3.431(5) | 1.7231481 | 1.7229734 | -3.40(57) | -5.656(23) |
| ScO($X^2\Sigma^+$) ^d | 4.55(8) | 1.66608(19) | - | - | - |
| VO($X^4\Sigma_{1/2}^-$) ^e | 3.355(14) | 1.5893(2) | - | - | - |

^a This work, but μ value taken from Steimle *et al.* [35]

^b Values taken from Beaton *et al.* [83], Lesarri *et al.* [84], and Suenram *et al.* [85]

^c Values taken from Lesarri *et al.* [84] and Suenram *et al.* [85]

^d Values taken from Childs *et al.* [86], Shirley *et al.* [87], and Mukund *et al.* [88]

^e Values taken from Flory *et al.* [89], Suenram *et al.* [90], and Huber *et al.* [91]

By taking a look at the rotational BO correction term Δ_{U01}^{A} (A = Ti, Zr, Hf) it can be seen (Tab. 4) that for titanium the value -8.253(24) is in absolute terms larger than those of the elements zirconium and hafnium being -4.872(39) and -3.40(57), respectively [84], i.e., with increasing row number, the rotational BO correction increases. The rotational BO correction term Δ_{U01}^{B} (B=oxygen) is similar to the values reported for ZrO and HfO. The magnitude of the BO correction term, see $(\dots)_{\text{BO}}$ term in Eq. 2a, scales with the inverse of the atomic mass, and its effect on the rotational constant B_0 for TiO is roughly 0.1%. The influence of the BO correction term on B_0 for TiO is ten times larger than for HfO.

An even larger effect of isotopic scaling shows the BO correction on the distortion term of the spin-orbit coupling A_{01} . For TiO the BO term increases the A_{01} value by around 0.6%. Unfortunately, no A_{01} -BO corrected values for other diatomic molecules with spin-orbit coupling are known and therefore a comparison with TiO is not possible.

The above mentioned Born-Oppenheimer breakdown corrections are crucial when predicting rotational constants (Tab. 5) and transition frequencies (Tab. 12) of isotopologues that are not easy to access via laboratory investigations. For example, astronomical searches for the short-lived ^{44}TiO isotopologue, expected to be present in supernovae remnants, require an accuracy in the sub-MHz range which is only feasible with consideration of the BO correction terms.

Finally, we compare the experimentally derived BO correction terms with those from theory. There, the corresponding values are $\Delta_{U01}^{\text{Ti}} = -4.9$ and $\Delta_{U01}^{\text{O}} = -6.7$. Thus, a rather good agreement is seen for the breakdown parameter of oxygen, while the experimentally determined parameter for titanium is significantly

Tab. 5: Predicted rotational parameter (in MHz) of the $X^3\Delta$ state of ^{44}TiO .

| ^{44}TiO | |
|-------------------------|-----------------|
| $T \cdot 10^{-7}$ | 1.5262874(8) |
| $B \cdot 10^{-4}$ | 1.636608750(37) |
| $D \cdot 10^2$ | 1.895723(78) |
| $H \cdot 10^9$ | 3.60(32) |
| $A \cdot 10^{-6}$ | 1.5184807(15) |
| $A_D \cdot 10^1$ | -8.4373(42) |
| $\lambda \cdot 10^{-4}$ | 5.23787(19) |
| $\lambda_D \cdot 10^2$ | 1.697(38) |

^a Values in brackets represents 1σ uncertainties.

larger than the computed one. However, it should be noted that the uncertainty in the theoretical value for titanium is rather high, e.g., using rotational g-tensors from CCSD instead of CCSD(T) computations changes the titanium parameter by roughly -0.8. Furthermore, the theoretical approach to the BO breakdown parameters does not consider spin-orbit effects and thus might be insufficient considering the large BO effect on the A_{01} term.

6.3. Electronic structure of ($X^3\Delta$) TiO

From the analysis of ^{47}TiO and ^{49}TiO the hyperfine (hf) parameters were derived, as given in Tab. 6. The hf values of the Frosch and Foley [92], i.e., the hyperfine constant b , as well as, the dipolar interaction constant c differ from those reported by Linkowski *et al.* [23]. However, we re-fitted the molecular parameters of the odd numbered TiO isotopologues with PGOPHER only by using their rotational transitions, which are in good agreement with the values derived from the mass-independent fitting routine, as can be seen in Tab. 6.

Anyway, the molecular hf parameters allow insights into the electronic structure of TiO. Four topics will be discussed in this section: The ionic vs. atomic character of the TiO bond, the contribution of the various atomic orbitals to the molecular bond, the dipole character of the molecular bond, and the localization of the bonding electrons. For further analysis of the electronic structure we apply the free atom comparison method (FACM)[27, 93, 94, 95] which makes use of the most dominant electronic configuration and its orbital model (details are given in the Appendix). For the first time, this analysis of the molecular structure of TiO is based only on experimental values.

Background. The electron configuration of the ground state $X^3\Delta$ can be qualitatively described as (core)(9σ)¹(1δ)¹, the open-shell electrons occupying the 9σ and the 1δ molecular orbital. Bauschlicher *et al.* [96] concluded in their theoretical study that the two unpaired electrons originate from the titanium. Namiki *et al.* [95] introduced a simple model for the unpaired electron orbitals, handling those molecular open-shell orbitals by describing them as a linear combination of titanium atomic/ionic orbitals.

Ionic vs. atomic character of the bond. Theoretical studies showed that the bonding of TiO is in between a covalent and an ionic one [96, 97]. The bond character is experimentally determined by using the FAC method together with the fine and hyperfine parameters of TiO, Ti, and Ti⁺. The nuclear spin-orbit interaction of a diatomic molecule can be expressed by

$$a = 2\mu_B g_N \mu_N \frac{\mu_0}{4\pi} \frac{1}{\Lambda} \langle \Lambda\Sigma | \sum_i \frac{\hat{l}_{zi}}{r_i^3} | \Lambda\Sigma \rangle \quad (4)$$

with the molecular nuclear spin-orbit constant a , the electron Bohr magneton μ_B , the nuclear g factor g_N , the nuclear Bohr magneton μ_N , the magnetic constant μ_0 , the Λ orbital quantum number of the electronic state and the z component of the one-electron orbital angular operator \hat{l}_{zi} of the electron in question. The expectation value from a σ -type orbital is zero, therefore only the 1δ electron of TiO in the electronic ground state contributes to the nuclear spin-orbit interaction: $a = a(1\delta)$. The character of the 1δ molecular orbital is defined by the titanium $3d$ orbital that, according to the FAC method, leads to an ionic character, i.e., a c_{ion} value above 0.7, more precisely, the c_{ion} coefficient can be calculated (see A.13 ff) via

$$a(^{47}\text{TiO}) = (1 - c_{ion}^2) a_{3d}^{01}(^{47}\text{Ti}) + c_{ion}^2 a_{3d}^{01}(^{47}\text{Ti}^+). \quad (5)$$

with $a_{3d}^{01}(X/X^+)$ being atomic/ionic nuclear spin-orbit coupling constant. The atomic [98] and ionic [99] parameters of titanium ($a_{3d}^{01}(\text{Ti})$, $a_{3d}^{01}(\text{Ti}^+)$) in the specific electronic configurations (Appendix) are derived from literature and are listed in Table 7. From our experimentally derived nuclear spin-orbit parameter $a(^{47}\text{TiO}) = -53.155(43)$ MHz, the ionic character of TiO is derived applying Eq. 5 which yields $c_{ion} = 0.799(151)$, a slightly more ionic character than the value of Namiki *et al.* [95], $c_{ion} = 0.789(4)$. The large uncertainty of the derived c_{ion} value is due to the uncertainty of the ionic nuclear spin-orbit parameter $a_{3d}^{01}(\text{Ti}^+)$, which was generally not considered in the work of Namiki *et al.* [94]. Alternatively, the ionic character of the TiO bond can be derived from the molecular spin-orbit fine-structure parameter A , in a similar way as the hyperfine parameter a is derived (see A.17 ff). By making use of the atomic and ionic fine structure parameters ζ_{3d} of titanium (see Tab. 7), we obtain an ionic character coefficient $c_{ion} = 0.813(56)$, which is slightly larger than the value obtained from $a(^{47}\text{TiO})$. In the proceeding analysis, we use the more accurate value derived from $A(^{47}\text{TiO})$. Furthermore, we used the c_{ion} parameter from our analysis, and atomic and ionic parameters from the literature to derive scaled molecular parameters, as given in Tab. 7.

Contribution of the atomic orbitals to the molecular bonding. A close look at the molecular Fermi-contact parameter $b_{\text{F}} (= b + c/3)$ reveals that the contribution from the 1δ electron is small compared to the 9σ orbital (39.5(37) MHz $>$ -718(33) MHz) (see [Appendix](#)). The σ character $c_{4s}^{9\sigma}$ of the 9σ orbital is evaluated by assuming that the non s -type atomic orbitals (p_{σ}, d_{σ}) are compensating each other (i.e., last two terms in [A.25](#) and [A.27](#) cancel out each other), and leads to the value of $c_{4s}^{9\sigma} = 0.868(20)$. This agrees well with the pronounced $4s$ orbital character of Namiki *et al.* [95] expressed by $c_{4s}^{9\sigma} = 0.895(1)$. The comparison of those two values shows that if we assume ‘no-other σ -type’ contribution to $c_{4s}^{9\sigma}$ we slightly underestimate the σ character of the $4s$ orbital. It can also be seen that our value has a large uncertainty compared to the one by Namiki *et al.*, referring to their neglect of experimental atomic/ionic uncertainties. The missing contributions to the 9σ molecular orbital from the non s -type atomic orbitals, i.e., p_{σ} and d_{σ} , are assumed to be equal, so that $(c_{3d_{\sigma}}^{9\sigma})^2 = (c_{4p_{\sigma}}^{9\sigma})^2 = 0.12(2)$. Furthermore, it follows, that the mixed Fermi-contact $4p$ parameter value is equal to the $3d$ one, but of opposite sign, i.e., $a_{3d}^{10}(\text{TiO}) = -a_{4p}^{10}(\text{TiO})$, see [A.25](#).

The dipole character of the molecular bond. The hyperfine molecular dipole interaction parameter c can be used to investigate the dipole character of the molecular bond, see [A.32](#) ff and specifically [A.36](#). From this it can be seen that the dipole character predominantly results from the $3d$ orbital term with 16.8(14) MHz being about 1.5 times larger than the $4p$ orbital term with 11.6(14) MHz. The mixed dipolar parameter for the $4p$ orbital $a_{4p}^{12}(\text{TiO})$ is then determined to be 157(29) MHz. Hence, the contribution of the $4p$ orbitals to the 9σ MO is not negligible.

In summary, it seems that the 9σ molecular orbital is pushed towards the titanium electrostatically due to the anionic character of the oxygen and mixes with the $4p$ and $3d$ atomic orbital of Ti. This can be described as a polarization effect that leads to an increased molecular dipole parameter c .

The localization of the bonding electrons between Ti and O. The electric quadrupole parameter eQq_0 originates from the electric-field gradient from all electrons within the molecule on the odd-numbered Ti nuclei. It can be thought to be build of two parts $eQq_0 = eQq_{0|\text{pol}} + eQq_{0|\text{el}}$, with $eQq_{0|\text{pol}}$ as the static polarization component caused by the bound σ -electrons and the $eQq_{0|\text{el}}$ term taking into account then the unpaired valence electrons. The dipole magnetic hyperfine value c from ^{47}TiO (see [Tab. 6](#)) can be used to determine the contribution of the valence electrons on the eQq_0 [100],

$$eQq_{0|\text{el}} = -2 \cdot \frac{2}{3} \cdot \frac{e^2 Q}{\epsilon_0 \mu_B \mu_N \mu_0} \cdot c. \quad (6)$$

For ^{47}TiO the electric quadrupole parameter eQq_0 is -54.612(10) MHz. The valence electrons contributes with a value of 89.2(7) MHz to the electric quadrupole parameter. Thus, the core polarization has to be negative with $eQq_{0|\text{pol}} = -143.8(7)$ MHz. This large polarization value, roughly three times larger than eQq_0 , indicates that the closed-shell σ -electrons are strongly effected by the unbound σ electron. The unbound

Tab. 6: Comparison of hyperfine parameter for ^{47}TiO and ^{49}TiO (all values in MHz).

| | ^{49}TiO | | | ^{47}TiO | | | |
|------------|---------------------------|------------------------|------------------------|---------------------------|------------------------|------------------------|------------------------|
| | This work | Prev. work | | This work | Prev. work | | |
| | Fit A | Re-fitted ^a | Exp. work ^a | Fit A | Re-fitted ^a | Exp. work ^a | Theo work ^b |
| a | -53.171(43) | -53.184(44) | -53.155(85) | -53.155(43) | -53.175(50) | -53.36(28) | -50 |
| Δa | -12.585(84) | -12.584(85) | -19.01(36) | -12.647(84) | -12.645(99) | -18.28(67) | |
| b | -259.91(24) | -259.93(28) | -232.94 | -259.95(28) | -259.83(24) | -235.3(2.1) | -343.1 |
| c | 28.10(24) | 28.09(22) | - | 28.09(19) | 27.75(34) | - | 21.3 ^d |
| $b + c$ | -231.813(83) ^c | -231.840(81) | -231.94(17) | -231.744(83) ^c | -231.790(90) | -232.19(46) | |
| c_D | -0.0986(29) | -0.0987(31) | - | -0.0996(30) | -0.0983(39) | - | |
| eQq_0 | -44.666(8) | -44.734(12) | -44.72(10) | -54.612(10) | -54.591(7) | -54.587(86) | |

^a Values taken from Lincowski *et al.* [23], also $(b + c)_D = -0.0178(15)$ MHz

^b Values taken from Fletcher *et al.* [27]

^c Correlation coefficient: -0.953074 ^d Assuming pure $3d_\delta$ electron from Ti

δ electron seems to compensate the electrostatic polarization effect of the particular values. By taking a look at the ScO and VO molecules, see Table 4, one notices that with increasing atomic number the absolute value of the electric quadrupole coupling decreases. Evaluation of the effect of the valence electrons $eQq_{0|\text{el}}$ for ScO (19.755(2) MHz), TiO, and VO(-22, 6(1) MHz) shows that a compensation of $eQq_{0|\text{pol}}$ with respect to the σ -like orbitals takes place. The compensation increases with increasing 1δ occupation thereby leading to smaller eQq_0 values. Comparing the electric quadrupole coupling parameter eQq_0 of TiO with those of ZrO ($eQq_0 = 150.5499(46)$ MHz, $Q=-0.176$ b) and HfO ($eQq_0 = -5952.865(11)$ MHz, $Q=3.365$ b) after division by the quadrupole moment, it can be seen that this quantity directly reflects the electric field gradient at the coupling nucleus[78]. The increasing field gradients from TiO over ZrO to HfO is in qualitative agreement with the steeper potential of the corresponding atoms caused by the larger proton number .

For the first time, a complete mass independent Dunham-type analysis of titanium monoxide for all stable titanium isotopologues has been performed. The accuracy of the measurements on six isotopologues allows for a detailed analysis of the influence of the atomic masses on the bond lengths. From the molecular hyperfine parameters of the odd-numbered titanium isotopes (^{47}Ti , ^{49}Ti) a detailed description of the electronic structure of TiO can be given based on measured spectroscopic parameters. The mass-invariant parameter set of TiO has been used to calculate molecular parameters for the ground state $X^3\Delta$ of ^{44}TiO . As a result from this Dunham-like analysis the line prediction accuracy of ^{44}TiO is better than 0.1 MHz in the frequency range below 400 GHz, see Tab. 5. Models of a core collapse event of a massive star (25 M_\odot) predict isotopic mass ratio of $^{48}\text{Ti}/^{44}\text{Ti} \approx 3$ [101]. If rotational transitions of the most abundant TiO isotopologue are observable in the environment of a SNR, then ^{44}TiO will also be provided that the age of the object is in the range of the half life of ^{44}Ti which is 60 years [19]. For objects like SN1987A, a supernova

Tab. 7: Atomic, ionic, and mixed parameters^d used to characterize TiO within the FAC method.

| | Ti ^a | Ti ⁺ ^b | TiO ^c |
|----------------------------------|-----------------|------------------------------|------------------|
| ζ_{3d} [cm ⁻¹] | 82.4(50) | 111(3) | 101.3(37) |
| a_{3d}^{01} [MHz] | -43.7(18) | -58.5(55) | -53.5(39) |
| a_{3d}^{12} [MHz] | -39.9(37) | -47.1(48) | -44.7(35) |
| a_{3d}^{10} [MHz] | 52.3(77) | 33.6(28) | 39.5(37) |
| a_{4s}^{10} [MHz] | -487(9) | -836(10) | -718(33) |

^a Value taken from Aydin *et al.*[98] with configuration ($3d^34s$)

^b Value taken from Bouazza [99]

^c Scaled by the derived ionic character $c_{ion} = 0.813(56)$

^d Spin-orbit coupling ($\vec{L}\vec{S}$): ζ_{xy} ; nuclear spin-orbit coupling ($\vec{I}\vec{L}$): a_{xy}^{01} ; spin-dipole coupling ($I_z S_z$): a_{xy}^{12} ; Fermi-contact term ($\vec{I}\vec{S}$): a_{xy}^{10}

remnant observed in 1987, these conditions may be fulfilled, whereas for the SNR Cas A, which occurred 335 years ago[102], the depletion of ⁴⁴TiO is significant and the isotopic ratio ⁴⁸Ti/⁴⁴Ti may be increased by factor of 50, excluding a strong observation of ⁴⁴TiO in this stellar object. Nevertheless, accurate rotational transition predications of rare isotopologues, like ⁴⁴TiO and ²⁶AlO [45], foster a dedicated astronomical search for these rare molecules, which may serve as a clock to determine the age of SNRs .

7. Acknowledgment

The authors thank C. Amiot for providing us with his experimental data. Also the authors thank E. Stachowska for discussing the former reported atomic/ionic titanium hyperfine parameters. The authors acknowledge funding through the DFG priority program 1573 (*Physics of the Interstellar Medium*) under grants GI 319/3-1, GI 319/3-2, GA 370/6-1, GA 370/6-2, and the University of Kassel through P/1052 Programmlinie *Zukunft*.

Tab. 8: Measured rotational transition frequencies (in MHz) of the $^3\Delta$ ground state of $^{46,48,50}\text{TiO}$. Experimental uncertainties are given in parentheses with 1σ deviation[103]. The weighted rms value is unitless.

| J'' | Ω'' | ^{46}TiO | o.-c. | ^{48}TiO | o.-c. | ^{50}TiO | o.-c. |
|--------------|------------|-------------------|--------|-------------------|--------|-------------------|--------|
| $\nu = 0$ | | | | | | | |
| 7 | 1 | 255943.678(50) | 0.061 | 253229.064(50) | 0.015 | 250728.856(50) | -0.028 |
| | 2 | 258927.037(100) | 0.023 | 256149.497(50) | -0.024 | 253592.150(150) | 0.157 |
| | 3 | 261511.461(100) | 0.080 | 258677.634(50) | 0.050 | 256068.870(50) | 0.085 |
| 8 | 1 | 287929.144(50) | -0.001 | 284875.296(50) | -0.043 | 282062.428(150) | -0.300 |
| | 2 | 291280.974(100) | 0.027 | 288156.474(50) | -0.058 | 285279.626(150) | 0.072 |
| | 3 | 294185.667(100) | -0.003 | 290998.150(50) | 0.123 | 288063.627(100) | 0.156 |
| 9 | 1 | 319912.095(100) | 0.061 | 316519.049(50) | 0.028 | 313393.923(50) | -0.077 |
| | 2 | 323630.596(100) | -0.073 | 320159.464(50) | 0.037 | 316963.264(150) | 0.179 |
| | 3 | 326854.831(150) | 0.025 | 323313.533(50) | 0.082 | 320053.306(150) | 0.049 |
| 10 | 1 | 351891.923(100) | -0.061 | 348159.793(50) | -0.005 | 344722.258(50) | -0.138 |
| | 2 | 355975.594(100) | -0.123 | 352157.711(50) | -0.038 | 348642.189(150) | 0.053 |
| | 3 | 359518.522(150) | 0.299 | 355623.365(50) | -0.063 | 352037.535(50) | -0.070 |
| 11 | 1 | 383868.657(50) | -0.034 | 379797.325(50) | -0.045 | 376047.589(100) | -0.033 |
| | 2 | ... | | 384151.007(50) | -0.038 | ... | |
| weighted rms | | | 0.878 | | 1.119 | | 1.318 |
| $\nu = 1$ | | | | | | | |
| 8 | 2 | ... | | 286512.767(100) | -0.008 | ... | |
| 9 | 2 | ... | | 318332.981(100) | 0.014 | ... | |
| weighted rms | | | | | 0.353 | | |

Tab. 9: Measured rotational transition frequencies (in MHz) of the $^3\Delta_1$ ground state of $^{48}\text{Ti}^{18}\text{O}$. Experimental uncertainties are given in parentheses with 1σ deviation[103]. The weighted rms value is unitless.

| J'' | Ω'' | $^{48}\text{Ti}^{18}\text{O}$ | o.-c. |
|--------------|------------|-------------------------------|--------|
| 8 | 1 | 261372.541(100) | -0.030 |
| 9 | 1 | 290405.742(100) | 0.030 |
| 10 | 1 | 319436.208(100) | -0.026 |
| 11 | 1 | 348463.857(100) | -0.012 |
| 12 | 1 | 377488.377(100) | 0.031 |
| weighted rms | | | 0.268 |

Tab. 10: Measured rotational transition frequencies (in MHz) of the $^3\Delta$ ground state of ^{47}TiO and ^{49}TiO . Experimental uncertainties are given in parentheses with 1σ deviation[103]. The weighted rms value is unitless.

| J'' | Ω'' | F'' | ^{47}TiO | o.-c. | ^{49}TiO | o.-c. |
|--------------|------------|-------|-------------------|--------|-------------------|--------|
| 7 | 1 | 10.5 | | | 251935.903(100) | 0.055 |
| | | 9.5 | 254544.359(100) | 0.072 | 251942.371(150) | 0.120 |
| | | 8.5 | 254550.242(100) | 0.088 | 251948.011(150) | 0.032 |
| | | 7.5 | 254555.313(150) | 0.023 | 251953.253(150) | 0.121 |
| | | 6.5 | 254559.961(150) | 0.048 | 251957.979(100) | 0.186 |
| | | 5.5 | 254564.283(150) | 0.088 | 251962.224(150) | 0.198 |
| | | 4.5 | 254568.345(150) | 0.082 | 251965.898(150) | 0.017 |
| | | 3.5 | | | 251969.486(150) | 0.099 |
| 2 | | 3.5 | | | ... | |
| | | 4.5 | 257495.492(150) | 0.090 | ... | |
| | | 5.5 | 257497.142(150) | 0.098 | ... | |
| | | 6.5 | 257500.228(150) | 0.217 | ... | |
| | | 7.5 | 257504.545(150) | 0.300 | ... | |
| | | 8.5 | 257509.880(150) | 0.219 | ... | |
| | | 9.5 | 257516.287(150) | 0.146 | ... | |
| | | 10.5 | | | ... | |
| 8 | 1 | 11.5 | | | 283423.732(100) | -0.040 |
| | | 10.5 | 286357.289(100) | 0.047 | 283429.209(100) | -0.052 |
| | | 9.5 | 286362.415(100) | 0.052 | 283434.410(100) | 0.149 |
| | | 8.5 | 286367.102(100) | 0.156 | 283438.860(150) | 0.012 |
| | | 7.5 | 286371.218(100) | 0.057 | 283443.147(150) | 0.059 |
| | | 6.5 | 286375.267(150) | 0.118 | 283447.094(150) | 0.059 |
| | | 5.5 | 286379.134(150) | 0.117 | 283450.880(100) | 0.150 |
| | | 4.5 | | | 283454.325(100) | 0.125 |
| 2 | | 4.5 | | | ... | |
| | | 5.5 | ... | | ... | |
| | | 6.5 | 289675.950(150) | 0.086 | ... | |
| | | 7.5 | 289678.518(150) | 0.176 | ... | |
| | | 8.5 | 289681.959(150) | 0.237 | ... | |
| | | 9.5 | 289686.450(500) | 0.531 | ... | |
| | | 10.5 | 289691.006(150) | 0.184 | ... | |
| | | 11.5 | | | ... | |
| 9 | 1 | 12.5 | | | 314908.843(100) | 0.072 |
| | | 11.5 | 318167.302(100) | -0.040 | 314913.733(100) | 0.094 |
| | | 10.5 | 318171.990(100) | 0.042 | 314918.150(100) | 0.013 |
| | | 9.5 | 318176.329(150) | 0.185 | 314922.381(100) | 0.051 |
| | | 8.5 | 318180.056(150) | -0.012 | 314926.379(100) | 0.109 |
| | | 7.5 | 318183.917(150) | 0.082 | 314930.155(100) | 0.155 |
| | | 6.5 | 318187.561(150) | 0.026 | 314933.611(100) | 0.055 |
| | | 5.5 | | | 314937.085(150) | 0.122 |
| 2 | | 5.5 | | | ... | |
| | | 6.5 | 321848.196(150) | -0.230 | ... | |
| | | 7.5 | 321849.698(150) | -0.098 | ... | |
| | | 8.5 | 321851.898(150) | 0.003 | ... | |
| | | 9.5 | 321854.838(150) | 0.179 | ... | |
| | | 10.5 | 321858.242(150) | 0.233 | ... | |
| | | 11.5 | 321862.056(150) | 0.210 | ... | |
| | | 12.5 | | | ... | |
| 10 | 1 | 13.5 | | | 346390.745(100) | 0.085 |
| | | 12.5 | 349974.347(100) | -0.018 | 346395.133(50) | 0.048 |
| | | 11.5 | 349978.609(150) | 0.009 | 346399.297(50) | 0.073 |
| | | 10.5 | 349982.608(150) | 0.094 | 346403.186(100) | 0.057 |
| | | 9.5 | 349986.306(150) | 0.086 | 346406.944(100) | 0.100 |
| | | 8.5 | 349989.799(150) | -0.016 | 346410.456(100) | 0.050 |
| | | 7.5 | 349993.386(150) | 0.010 | 346414.006(100) | 0.162 |
| | | 6.5 | | | 346417.076(150) | -0.105 |
| 11 | 1 | 14.5 | | | 377869.209(50) | -0.001 |
| | | 13.5 | 381778.101(100) | 0.044 | 377873.306(100) | 0.000 |
| | | 12.5 | 381782.089(100) | 0.074 | 377877.209(100) | 0.032 |
| | | 11.5 | 381785.732(100) | 0.018 | 377880.886(100) | 0.021 |
| | | 10.5 | 381789.331(100) | 0.079 | 377884.429(100) | 0.022 |
| | | 9.5 | 381792.822(100) | 0.112 | 377887.907(100) | 0.073 |
| | | 8.5 | 381796.210(100) | 0.056 | 377891.287(100) | 0.116 |
| | | 7.5 | | | 377894.463(100) | 0.024 |
| weighted rms | | | | 0.999 | | 0.920 |

Tab. 11: Mass-invariant molecular parameters based on the analysis of six stable titanium isotopologues, $^{46-50}\text{Ti}^{16}\text{O}$ and $^{48}\text{Ti}^{18}\text{O}$.

| Parameter ^a | This work | | Prev. work | | Units |
|--------------------------------|--------------------|--------------------|---------------|------------------------|----------------------------------------------------------------|
| | Fit A ^b | Fit B ^c | Re-Fitted | published ^d | |
| X ³ Δ state | | | | | |
| U_{00} | 0.0 | 0.0 | 0.0 | 0.0 | cm ⁻¹ |
| $U_{10} \cdot 10^{-3}$ | 3.4949966(26) | 3.4949959(26) | 3.4949984(29) | 3.4949989(23) | cm ⁻¹ u ^{1/2} |
| $U_{20} \cdot 10^{-1}$ | -5.47093(45) | -5.47063(46) | -5.47110(46) | -5.47129(36) | cm ⁻¹ u |
| $U_{30} \cdot 10^1$ | -1.587(22) | -1.596(22) | -1.582(22) | -1.571(18) | cm ⁻¹ u ^{3/2} |
| U_{01} | 6.4227037(25) | 6.4234987(74) | 6.4207505(16) | 6.4207506(20) | cm ⁻¹ u |
| Δ_{01}^T | -8.253(24) | -8.282(25) | - | - | |
| Δ_{01}^O | -6.112(8) | -9.722(29) | - | - | |
| $U_{11} \cdot 10^1$ | -1.255825(44) | -1.255631(69) | -1.25598(11) | -1.25599(15) | cm ⁻¹ u ^{3/2} |
| $U_{21} \cdot 10^3$ | -1.3467(57) | -1.3542(61) | -1.3399(71) | -1.325(13) | cm ⁻¹ u ² |
| $U_{02} \cdot 10^5$ | 8.67195(38) | 8.67186(38) | 8.6636(18) | 8.6647(13) | cm ⁻¹ u ² |
| $U_{12} \cdot 10^6$ | 1.7341(67) | 1.7469(81) | 1.7198(120) | 1.701(32) | cm ⁻¹ u ^{5/2} |
| $U_{03} \cdot 10^{10}$ | 1.95(17) | 2.05(17) | 1.17(24) | 1.19(28) | cm ⁻¹ u ³ |
| $A_{00} \cdot 10^{-1}$ | 5.065030(11) | 5.064254(14) | 5.065029(11) | 5.065041(10) | cm ⁻¹ |
| $A_{10} \cdot 10^3$ | 6.77(73) | 4.93(84) | 6.74(73) | 6.70(58) | cm ⁻¹ u ^{1/2} |
| $A_{20} \cdot 10^3$ | -10.61(51) | -10.88(53) | -10.57(51) | -10.10(42) | cm ⁻¹ u |
| $A_{01} \cdot 10^4$ | -1.797(10) | 1.722(56) | -3.1136(36) | -3.1080(32) | cm ⁻¹ u |
| $\Delta_{A01}^T \cdot 10^{-4}$ | 6.429(85) | - | - | - | |
| $A_{11} \cdot 10^5$ | -4.25(22) | 7.3(28) | -4.28(22) | -4.58(22) | cm ⁻¹ u ^{3/2} |
| $\gamma_{01} \cdot 10^2$ | - | 9.00(10) | - | - | cm ⁻¹ u |
| $\gamma_{11} \cdot 10^2$ | - | 2.36(52) | - | - | cm ⁻¹ u ^{3/2} |
| λ_{00} | 1.74974(16) | 1.74584(18) | 1.74970(16) | 1.74991(14) | cm ⁻¹ |
| $\lambda_{10} \cdot 10^2$ | -1.81(11) | -2.00(12) | -1.84(12) | -1.88(9) | cm ⁻¹ u ^{1/2} |
| $\lambda_{20} \cdot 10^3$ | 3.19(85) | 3.13(85) | 3.37(86) | 3.60(68) | cm ⁻¹ u |
| $\lambda_{01} \cdot 10^6$ | 6.64(15) | -47.76(44) | 7.81(27) | 8.06(19) | cm ⁻¹ u ^{3/2} |
| $a_{00} \cdot 10^3$ | 5.6220(45) | 5.6133(46) | - | - | cm ⁻¹ g _N ⁻¹ |
| $\Delta a_{00} \cdot 10^3$ | 4.620(31) | 4.684(31) | - | - | cm ⁻¹ g _N ⁻¹ u ^{1/2} |
| $b_{00} \cdot 10^2$ | 2.7481(30) | 2.7653(26) | - | - | cm ⁻¹ g _N ⁻¹ |
| $c_{00} \cdot 10^3$ | -2.971(20) | -3.160(20) | - | - | cm ⁻¹ g _N ⁻¹ |
| $c_{01} \cdot 10^4$ | 1.257(37) | 1.205(38) | - | - | cm ⁻¹ g _N ⁻¹ u |
| $eQq_{000} \cdot 10^3$ | -6.0320(11) | -6.0322(11) | - | - | cm ⁻¹ b ⁻¹ |
| weighted rms | 1.00 | 1.01 | 1.00 | 1.10 | |
| unweighted rms | 0.00547 | 0.00550 | 0.00577 | 0.0054 | cm ⁻¹ |

^a Mass-invariant molecular parameters of the electronic states A³Φ and B³Π are listed in the supplementary material.

^b Fit A uses the same parameter set as Ram *et al.* [26].

^c Fit B includes the spin-rotational parameters: $\gamma = \gamma_{01}\mu^{-1} + 0.5\gamma_{11}\mu^{-1.5}$

^d Values taken from Ram *et al.* [26] and scaled mass-independent values using $\mu^{48}\text{Ti}^{16}\text{O} = 11.99388479(6)\text{u}$. Also reported parameter $U_{22} = 5.5(31) \cdot 10^{-8}\text{cm}^{-1}\text{u}^6$.

Tab. 12: Predicted rotational transition frequencies (in MHz) of the ${}^3\Delta_1$ ground state of ${}^{44}\text{TiO}$ and even titanium isotopologues.

| J'' | ${}^{44}\text{TiO}$ |
|-------|---------------------|
| 1 | 64730.891(3) |
| 2 | 97095.606(4) |
| 3 | 129459.442(6) |
| 4 | 161822.105(7) |
| 5 | 194183.299(9) |
| 6 | 226542.728(10) |
| 7 | 258900.092(12) |
| 8 | 291255.091(13) |
| 9 | 323607.420(15) |
| 10 | 355956.774(16) |
| 11 | 388302.843(18) |
| 12 | 420645.312(19) |

^a Frequency uncertainties are obtained by empirical variation of molecular parameter uncertainties.

Tab. 13: Measured rotational transition frequencies (in MHz) of the ground state of ${}^{48}\text{TiO}_2$. Experimental uncertainties are given in parentheses with 1σ deviation [103]. For comparison, the calculated values and uncertainties given in the CDMS are also listed[104].

| $\Delta^K \Delta J_{K_a'', K_c''}(J'')$ | This work | CDMS[104] |
|-----------------------------------------|-----------------|----------------|
| ${}^r Q_{5,3}(7)$ | 251977.114(50) | 251977.193(11) |
| ${}^r R_{2,18}(19)$ | 283567.854(50) | 283567.716(22) |
| ${}^r Q_{6,4}(10)$ | 297418.481(50) | 297418.556(10) |
| ${}^r Q_{6,4}(9)$ | 297539.720(50) | 297539.750(11) |
| ${}^p R_{1,21}(21)$ | 297553.693(100) | 297553.951(50) |
| ${}^r Q_{6,2}(8)$ | 297623.750(50) | 297623.702(13) |
| ${}^r Q_{6,2}(7)$ | 297678.435(50) | 297678.543(16) |

8. References

References

- [1] A. Fowler, *Proc. R. Soc. London* 73 (1904) 219.
- [2] P. W. Merrill, A. J. Deutsch, P. C. Keenan, *Astrophys. J.* 136 (1962) 21.
- [3] T. Kamiński, C. A. Gottlieb, K. M. Menten, N. A. Patel, K. H. Young, S. Brünken, H. S. P. Müller, M. C. McCarthy, J. M. Winters, L. Decin, *Astron. Astrophys.* 551 (2013) A113.
- [4] P. Kervella, E. Lagarde, M. Montargès, S. T. Ridgway, A. Chiavassa, X. Haubois, H.-M. Schmid, M. Langlois, A. Gallenne, G. Perrin, *Astron. Astrophys.* 585 (2016) A28.
- [5] T. Kamiński, H. S. P. Müller, M. R. Schmidt, I. Cherchneff, K. T. Wong, S. Brünken, K. M. Menten, J. M. Winters, C. A. Gottlieb, N. A. Patel, *Astron. Astrophys.* 599 (2017) A59.
- [6] W. W. Morgan, P. C. Keenan, *Annu. Rev. Astron. Astrophys.* 11 (1973) 29.
- [7] T. Tsuji, *Annu. Rev. Astron. Astrophys.* 24 (1986) 89.
- [8] R. P. Schiavon, B. Barbuy, *Astrophys. J.* 510 (1999) 934.
- [9] J. J. Fortney, K. Lodders, M. S. Marley, R. S. Freedman, *Astrophys. J.* 678 (2008) 1419.
- [10] T. M. Evans, D. K. Sing, H. R. Wakeford, N. Nikolov, G. E. Ballester, Benjamin Drummond, T. Kataria, N. P. Gibson, D. S. Amundsen, J. Spake, *Astrophys. J. Lett.* 822 (2016) L4.
- [11] J. Tennyson, S. N. Yurchenko, A. F. Al-Refaie, E. J. Barton, K. L. Chubb, P. A. Coles, S. Diamantopoulou, M. N. Gorman, C. Hill, A. Z. Lam, L. Lodi, L. K. McKemmish, Y. Na, A. Owens, O. L. Polyansky, T. Rivlin, C. Sousa-Silva, D. S. Underwood, A. Yachmenev, E. Zak, *J. Mol. Spectrosc.* 327 (2016) 73.
- [12] E. Sedaghati, H. M. J. Boffin, R. J. MacDonald, S. Gandhi, N. Madhusudhan, N. P. Gibson, M. Oshagh, A. Claret, H. Rauer, *Nature* 549 (2017) 238.
- [13] F. X. Timmes, S. E. Woosley, D. H. Hartmann, R. D. Hoffman, *Astrophys. J.* 464 (1996) 332.
- [14] Y.-H. Lee, B.-C. Koo, D.-S. Moon, M. G. Burton, J.-J. Lee, *Astrophys. J.* 837 (2017) 118.
- [15] A. F. Iyudin, V. Schönfelder, K. Bennett, H. Bloemen, R. Diehl, W. Hermsen, G. G. Lichti, R. D. van der Meulen, J. Ryan, C. Winkler, *Nature* 396 (1998) 142.
- [16] S. S. Tsygankov, R. A. Krivonos, A. A. Lutovinov, M. G. Revnivtsev, E. M. Churazov, R. A. Sunyaev, S. A. Grebenev, *Mon. Not. R. Astron. Soc.* 458 (2016) 3411.
- [17] A. Wongwathanarat, H.-T. Janka, E. Müller, E. Pllumbi, S. Wanajo, *Astrophys. J.* 842 (2017) 13.
- [18] S. Boggs, F. Harrison, H. Miyasaka, B. Grefenstette, A. Zoglauer, C. Fryer, S. Reynolds, D. M. Alexander, H. An, D. Barret, F. E. Christensen, W. W. Craig, K. Forster, P. Giommi, C. J. Hailey, A. Hornstrup, T. Kitaguchi, J. E. Koglin, K. K. Madsen, P. H. Mao, K. Mori, M. Perri, M. J. Pivovarov, S. Puccetti, V. Rana, D. Stern, N. J. Westergaard, W. W. Zhang, *Science* 348 (2015) 670.
- [19] I. Ahmad, J. P. Greene, E. F. Moore, S. Ghelberg, A. Ofan, M. Paul, W. Kutschera, *Phys. Rev. C: Nucl. Phys.* 74 (2006) 065803.
- [20] J. L. Dunham, *Phys. Rev.* 41 (1932) 721.
- [21] J. Van Vleck, *J. Chem. Phys.* 4 (1936) 327.
- [22] A. Christy, *Phys. Rev.* 33 (1929) 701.
- [23] A. P. Lincowski, D. T. Halfen, L. M. Ziurys, *Astrophys. J.* 833 (2016) 9.
- [24] L. K. McKemmish, T. Masseron, S. Sheppard, E. Sandeman, Z. Schofield, T. Furtenbacher, A. G. Császár, J. Tennyson, C. Sousa-Silva, *Astrophys. J. Suppl. Ser* 228 (2017) 15.
- [25] C. Amiot, E. M. Azaroual, P. Luc, R. Vetter, *J. Chem. Phys.* 102 (1995) 4375.
- [26] R. S. Ram, P. F. Bernath, M. Dulick, L. Wallace, *Astrophys. J. Suppl. Ser* 122 (1999) 331.

- [27] D. A. Fletcher, C. T. Scurlock, K. Y. Jung, T. C. Steimle, *J. Chem. Phys.* 99 (1993) 4288.
- [28] M. Barnes, A. Merer, G. Metha, *J. Mol. Spectrosc.* 180 (1996) 437.
- [29] C. Amiot, P. Luc, R. Vetter, *J. Mol. Spectrosc.* 214 (2002) 196.
- [30] K. Kobayashi, G. E. Hall, J. T. Muckerman, T. J. Sears, A. J. Merer, *J. Mol. Spectrosc.* 212 (2002) 133.
- [31] K. Namiki, S. Saito, J. Robinson, T. C. Steimle, *J. Mol. Spectrosc.* 191 (1998) 176.
- [32] P. Kania, T. F. Giesen, H. S. P. Müller, S. Schlemmer, S. Brünken, in: [2008 33rd International Conference on Infrared, Millimeter and Terahertz Waves](#), p. 1.
- [33] A. J. Merer, *Annu. Rev. Phys. Chem.* 40 (1989) 407.
- [34] A. J. Bridgeman, J. Rothery, *J. Chem. Soc., Dalton Trans.* (2000) 211.
- [35] T. C. Steimle, W. Virgo, *Chem. Phys. Lett.* 381 (2003) 30.
- [36] A. A. Breier, T. Büchling, R. Schnierer, V. Lutter, G. W. Fuchs, K. M. T. Yamada, B. Mookerjea, J. Stutzki, T. F. Giesen, *J. Chem. Phys.* 145 (2016) 234302.
- [37] P. Neubauer-Guenther, T. Giesen, U. Berndt, G. Fuchs, G. Winnewisser, *Spectrochim. Acta, Part A* 59 (2003) 431.
- [38] M. Shima, N. Torigoye, *Int. J. Mass Spectrom. Ion Processes* 123 (1993) 29.
- [39] J. Meija, T. B. Coplen, M. Berglund, W. A. Brand, P. De Bièvre, M. Gröning, N. E. Holden, J. Irrgeher, R. D. Loss, T. Walczyk, et al., *Pure Appl. Chem.* 88 (2016) 293.
- [40] R. J. Le Roy, *J. Mol. Spectrosc.* 191 (1998) 223.
- [41] C. M. Western, *J. Quant. Spectrosc. Radiat. Transfer* (2011).
- [42] J. K. G. Watson, *J. Mol. Spectrosc.* 45 (1973) 99.
- [43] A. H. M. Ross, R. S. Eng, H. Kildal, *Opt. Commun.* 12 (1974) 433.
- [44] J. K. G. Watson, *J. Mol. Spectrosc.* 80 (1980) 411.
- [45] A. A. Breier, B. Waßmuth, T. Büchling, G. W. Fuchs, J. Gauss, T. F. Giesen, *J. Mol. Spectrosc.* 350 (2018) 43.
- [46] H. S. P. Müller, K. Kobayashi, K. Takahashi, K. Tomaru, F. Matsushima, *J. Mol. Spectrosc.* 310 (2015) 92.
- [47] V. Lattanzi, G. Cazzoli, C. Puzzarini, *Astrophys. J.* 813 (2015) 4.
- [48] N. J. Stone, *At. Data Nucl. Data Tables* 90 (2005) 75.
- [49] R. K. Harris, E. D. Becker, d. M. S. M. Cabral, R. Goodfellow, P. Granger, *Pure Appl. Chem.* 73 (2009) 1795.
- [50] P. Pyykkö, *Mol. Phys.* 106 (2008) 1965.
- [51] J. M. Brown, J. K. Watson, *J. Mol. Spectrosc.* 65 (1977) 65.
- [52] M. Wang, G. Audi, F. Kondev, W. Huang, S. Naimi, X. Xu, *Chinese Phys. C* 41 (2017) 030003.
- [53] I. Shavitt, R. J. Bartlett, *Many-body methods in chemistry and physics: MBPT and coupled-cluster theory*, Cambridge university press, 2009.
- [54] T. H. Dunning Jr., *J. Chem. Phys.* 90 (1989) 1007.
- [55] M. Heckert, M. Kállay, J. Gauss, *Mol. Phys.* 103 (2005) 2109.
- [56] M. Heckert, M. Kállay, D. P. Tew, W. Klopper, J. Gauss, *J. Chem. Phys.* 125 (2006) 044108.
- [57] D. Feller, *J. Chem. Phys.* 98 (1993) 7059.
- [58] K. A. Peterson, T. H. Dunning Jr., *J. Chem. Phys.* 117 (2002) 10548.
- [59] N. B. Balabanov, K. A. Peterson, *J. Chem. Phys.* 123 (2005) 064107.
- [60] K. Raghavachari, G. W. Trucks, J. A. Pople, M. Head-Gordon, *Chem. Phys. Lett.* 157 (1989) 479.
- [61] T. Helgaker, W. Klopper, H. Koch, J. Noga, *J. Chem. Phys.* 106 (1997) 9639.
- [62] J. D. Watts, R. J. Bartlett, *J. Chem. Phys.* 93 (1990) 6104.
- [63] M. Kállay, P. R. Surján, *J. Chem. Phys.* 115 (2001) 2945.
- [64] K. G. Dyall, *J. Chem. Phys.* 106 (1997) 9618.
- [65] W. Kutzelnigg, W. Liu, *J. Chem. Phys.* 123 (2005) 241102.

- [66] M. Iliáš, T. Saue, *J. Chem. Phys.* 126 (2007) 064102.
- [67] L. Cheng, J. Gauss, *J. Chem. Phys.* 135 (2011) 084114.
- [68] B. O. Roos, R. Lindh, P.-Å. Malmqvist, V. Veryazov, P.-O. Widmark, *J. Phys. Chem. A* 108 (2004) 2851.
- [69] B. O. Roos, R. Lindh, P.-Å. Malmqvist, V. Veryazov, P.-O. Widmark, *J. Phys. Chem. A* 109 (2005) 6575.
- [70] J. Gauss, C. Puzzarini, *Mol. Phys.* 108 (2010) 269.
- [71] C. Puzzarini, J. Gauss, *Mol. Phys.* 111 (2013) 2204.
- [72] J. Gauss, K. Ruud, M. Kállay, *J. Chem. Phys.* 127 (2007) 074101.
- [73] D. E. Woon, T. H. Dunning Jr., *J. Chem. Phys.* 98 (1993) 1358.
- [74] J. Gauss, A. Tajti, M. Kállay, J. F. Stanton, P. G. Szalay, *J. Chem. Phys.* 125 (2006) 144111.
- [75] J. F. Stanton, J. Gauss, L. Cheng, M. E. Harding, D. A. Matthews, P. G. Szalay, CFOUR, Coupled-Cluster techniques for Computational Chemistry, a quantum-chemical program package, ????. With contributions from A.A. Auer, R.J. Bartlett, U. Benedikt, C. Berger, D.E. Bernholdt, S. Blaschke, Y. J. Bomble, S. Burger, O. Christiansen, D. Datta, F. Engel, R. Faber, J. Greiner, M. Heckert, O. Heun, M. Hilgenberg, C. Huber, T.-C. Jagau, D. Jonsson, J. Jusélius, T. Kirsch, K. Klein, G.M. KopperW.J. Lauderdale, F. Lipparini, T. Metzroth, L.A. Mück, D.P. O'Neill, T. Nottoli, D.R. Price, E. Prochnow, C. Puzzarini, K. Ruud, F. Schiffmann, W. Schwalbach, C. Simmons, S. Stopkowitz, A. Tajti, J. Vázquez, F. Wang, J.D. Watts and the integral packages MOLECULE (J. Almlöf and P.R. Taylor), PROPS (P.R. Taylor), ABACUS (T. Helgaker, H.J. Aa. Jensen, P. Jørgensen, and J. Olsen), and ECP routines by A. V. Mitin and C. van Wüllen. For the current version, see <http://www.cfour.de>.
- [76] A. Kratzer, *Z. Physik* 3 (1920) 289.
- [77] C. L. Pekeris, *Phys. Rev.* 45 (1934) 98.
- [78] W. Gordy, R. L. Cook, *Microwave molecular spectra*, Wiley, 1984.
- [79] P. M. Morse, *Phys. Rev.* 34 (1929) 57.
- [80] C. Naulin, I. M. Hedgecock, M. Costes, *Chem. Phys. Lett.* 266 (1997) 335.
- [81] R. R. Reddy, Y. N. Ahammed, K. R. Gopal, P. A. Azeem, T. V. R. Rao, *J. Quant. Spectrosc. Radiat. Transfer* 66 (2000) 501.
- [82] C. Puzzarini, J. F. Stanton, J. Gauss, *Int. Rev. Phys. Chem.* 29 (2010) 273.
- [83] S. A. Beaton, M. C. L. Gerry, *J. Chem. Phys.* 110 (1999) 10715.
- [84] A. Lesarri, R. D. Suenram, D. Brugh, *J. Chem. Phys.* 117 (2002) 9651.
- [85] R. D. Suenram, F. J. Lovas, G. T. Fraser, K. Matsumura, *J. Chem. Phys.* 92 (1990) 4724.
- [86] W. J. Childs, T. C. Steimle, *J. Chem. Phys.* 88 (1988) 6168.
- [87] J. Shirley, C. Scurlock, T. Steimle, *J. Chem. Phys.* 93 (1990) 1568.
- [88] S. Mukund, S. Yarlagadda, S. Bhattacharyya, S. G. Nakhate, *J. Quant. Spectrosc. Radiat. Transfer* 113 (2012) 2004.
- [89] M. A. Flory, L. M. Ziurys, *J. Mol. Spectrosc.* 247 (2008) 76.
- [90] R. D. Suenram, G. T. Fraser, F. J. Lovas, C. W. Gillies, *J. Mol. Spectrosc.* 148 (1991) 114.
- [91] K. Huber, G. Herzberg, *Molecular Spectra and Molecular Structure: IV. Constants of Diatomic Molecules*, Springer Science & Business Media, 1979.
- [92] R. A. Frosch, H. M. Foley, *Phys. Rev.* 88 (1952) 1337.
- [93] K. Namiki, H. Ito, *J. Mol. Spectrosc.* 214 (2002) 188.
- [94] K. Namiki, H. Miki, H. Ito, *Chem. Phys. Lett.* 370 (2003) 62.
- [95] K. Namiki, H. Saitoh, H. Ito, *J. Mol. Spectrosc.* 226 (2004) 87.
- [96] C. W. Bauschlicher, P. S. Bagus, C. J. Nelin, *Chem. Phys. Lett.* 101 (1983) 229.
- [97] C. W. Bauschlicher, P. Maitre, *Theoret. Chim. Acta* 90 (1995) 189.
- [98] R. Aydin, E. Stachowska, U. Johann, J. Dembczyński, P. Unkel, W. Ertmer, *Z. Phys. D: At., Mol. Clusters* 15 (1989)

- [99] S. Bouazza, *Phys. Scr.* 87 (2013) 045301.
- [100] C. Ryzlewicz, H.-U. Schütze-Pahlmann, J. Hoeft, T. Törring, *Chem. Phys.* 71 (1982) 389.
- [101] B. S. Meyer, T. A. Weaver, S. E. Woosley, *Meteoritics* 30 (1995) 325.
- [102] R. A. Fesen, M. C. Hammell, J. Morse, R. A. Chevalier, K. J. Borkowski, M. A. Dopita, C. L. Gerardy, S. S. Lawrence, J. C. Raymond, S. van den Bergh, *Astrophys. J.* 645 (2006) 283.
- [103] ???? To take systematic error into account we used the following procedure by linking the experimental frequency uncertainty to the signal-to-noise ratios (SNR): SNR > 10: 50 kHz, SNR > 5: 100 kHz, and SNR < 5: 150 kHz.
- [104] C. P. Endres, S. Schlemmer, P. Schilke, J. Stutzki, H. S. Müller, *J. Mol. Spectrosc.* 327 (2016) 95.
- [105] E. Stachowska, *Z. Phys. D: At., Mol. Clusters* 42 (1997) 33.

Appendix

A. FACM on $(X^3\Delta)TiO$

The free atomic comparison method (FACM) is used to evaluate the electronic ground state of TiO, based on the electronic molecular configuration:

$$X^3\Delta : (core)(9\sigma)^1(1\delta^+)^1 \quad \text{with} \quad (core) = (1\sigma)^2 - (8\sigma)^2(1\pi)^4 - (3\pi)^4. \quad (\text{A.1})$$

Theoretical predictions from Bauschlicher *et al.* [96] reveal a polarization of the titanium atom. The 9σ molecular orbital is electrostatically pushed away from the oxygen and mixes with $4p$ and $3d$ atomic orbitals of titanium. Hence, the unpaired molecular orbitals (see Eq.(A.1)) are in good approximation linear combinations of $4s$, $4p$, and $3d$ orbitals of titanium. The small contribution of the oxygen $2p$ orbitals can be neglected and the σ orbital can be expressed as,

$$|9\sigma\rangle = c_{4s}^{9\sigma} |4s\rangle - c_{3d}^{9\sigma} |3d_\sigma\rangle - c_{4p}^{9\sigma} |4p_\sigma\rangle, \quad (\text{A.2})$$

$$(\text{A.3})$$

with the normalization $(c_{4s}^{9\sigma})^2 + (c_{3d_\sigma}^{9\sigma})^2 + (c_{4p_\sigma}^{9\sigma})^2 = 1$. The 1δ molecular orbital is well represented by the $3d$ Ti orbital,

$$|1\delta\rangle = |3d_\delta\rangle. \quad (\text{A.4})$$

The TiO bond is thought of being partly covalent and ionic character. This assumption is based on the electron donation in TiO [96]. The atomic orbital can be described as

$$|\chi\rangle = c_{atom}^2 |\chi(Ti)\rangle + c_{ion}^2 |\chi(Ti^+)\rangle \quad (\text{A.5})$$

utilizing the normalization relation $c_{atom}^2 + c_{ion}^2 = 1$. The FAC method makes use of the atomic fine- and hyperfine-structure parameters. Therefore, this method balances the molecular-orbital properties by the

atomic and ionic structure parameters. In the further description the parameters derived from Eq.(A.5) are called ‘mixed parameter values’. In this paper, we use the model-space parameter description $(3d + 4s)^{N+2}$ of Ti ($N = 2$) [98], or Ti^+ ($N = 1$) [99]. Where the one-body-parameter $a_{nl}^{\kappa k}(l^{N+M}s^{2-M})$ are related to the model-space parameters $a_{nl}^{\kappa k}$,

$$a_{nl}^{\kappa k}(l^{N+M}s^{2-M}) = a_{nl}^{\kappa k} + \frac{2}{2l+1}(1-N-M)a_1 - \sqrt{\frac{2}{2l+1}}(2-M)a_4 + \frac{2}{2l+1}a_5\delta(M, 0), \quad (\text{A.6})$$

for $\kappa k = 01, 12$. In the case of $\kappa k = 10$ it follows:

$$\begin{aligned} a_{nl}^{10}(l^{N+1}s^1) &= a_{nl}^{10} - \frac{2}{2l+1}a_9, \\ a_{nl}^{10}(l^{N+2}) &= a_{nl}^{10} - \frac{2}{2l+1}(a_{10} - a_9). \end{aligned} \quad (\text{A.7})$$

In the case of atomic Ti and ionic Ti^+ we use the electronic configuration $(3d^3s^1)$ and $(3d^2s^1)$, respectively, within the model space. It represents the donation of unbound TiO electrons originating from the Ti atom. Therefore in case of titanium, the Eq. (A.6) and (A.7) reduce to the following expressions for the atomic/ionic parameters

$$a_{3d}^{\kappa k}(3d^34s^1) = a_{3d}^{\kappa k} - \frac{4}{5}a_1, \quad (\text{A.8})$$

$$a_{3d}^{10}(3d^34s^1) = a_{3d}^{10} - \frac{2}{5}a_9, \quad (\text{A.9})$$

and in case of Ti^+ we write

$$a_{3d}^{\kappa k}(3d^2s^1) = a_{3d}^{\kappa k} - \frac{2}{5}a_1, \quad (\text{A.10})$$

$$a_{3d}^{10}(3d^2s^1) = a_{3d}^{10} - \frac{2}{5}a_9. \quad (\text{A.11})$$

First, we want to determine the ionic character for the ground state $X^3\Delta$ of TiO. A convenient way to calculate the ionic character is by using the molecular hyperfine nuclear spin-orbit coupling parameter a , as defined by

$$a = 2\mu_B g_N \mu_N \frac{\mu_0}{4\pi} \frac{1}{\Lambda} \langle \Lambda \Sigma | \sum_i \frac{\hat{l}_{zi}}{r_i^3} | \Lambda \Sigma \rangle, \quad (\text{A.12})$$

with the electron Bohr magneton μ_B , the nuclear Bohr magneton μ_N , the nuclear g factor g_N , the magnetic constant μ_0 and the z component of the one-electron orbital angular operator \hat{l}_{zi} . The expectation value from a σ -type orbital is zero. Therefore only the 1δ electron of TiO in the electronic ground state will contribute to the nuclear spin-orbit interaction: $a = a(1\delta)$. This leads to

$$a = a(1\delta) = c_{atom}^2 \overbrace{a_{3d\delta}^{01}(Ti)} + c_{ion}^2 \overbrace{a_{3d\delta}^{01}(Ti^+)} \quad (\text{A.13})$$

$$= (1 - c_{ion}^2)a_{3d}^{01}(Ti) + c_{ion}^2 a_{3d}^{01}(Ti^+) \quad (\text{A.14})$$

$$\rightarrow c_{ion}^2 = \frac{a - a_{3d}^{01}(Ti)}{a_{3d}^{01}(Ti^+) - a_{3d}^{01}(Ti)} \quad (\text{A.15})$$

$$= 0.638(242) \quad (\text{A.16})$$

Another way to calculate the ionic character is to make use of the molecular fine structure, by using the spin-orbit parameter A ,

$$A = \frac{1}{\Lambda\Sigma} \langle \Lambda\Sigma | \sum_i \hat{a}_i \hat{l}_{zi} | \Lambda\Sigma \rangle, \quad (\text{A.17})$$

which for TiO results in,

$$A = 1/2 \langle 1\delta | \hat{a}_\delta \hat{l}_z | 1\delta \rangle \quad (\text{A.18})$$

$$\text{using Eq. (A.4) \& (A.13)} \rightarrow 2A = c_{atom}^2 \overbrace{A_{3d^3}(Ti)}^{\zeta_{3d}(Ti)} + c_{ion}^2 \overbrace{A_{3d^3}(Ti^+)}^{\zeta_{3d}(Ti^+)}. \quad (\text{A.19})$$

Furthermore, we use the atomic Ti spin-orbit parameter $\zeta_{3d}(Ti) = \zeta_{3d}(3d^34s^1) = 82.4(50) \text{ cm}^{-1}$ [105] and the ionic Ti with $\zeta_{3d}(Ti^+) = \zeta_{3d}(3d^24s^1) = 111(30) \text{ cm}^{-1}$ [99] within our FAC method. Determining the ionic character results in a value of

$$c_{ion}^2 = \frac{2A - \zeta_{3d}(Ti)}{\zeta_{3d}(Ti^+) - \zeta_{3d}(Ti)} \quad (\text{A.20})$$

$$= 0.661(91). \quad (\text{A.21})$$

The ionic character of TiO derived from the fine-structure parameter A with a value of 0.661(91) is in excellent agreement with the value extracted from the hyperfine parameter a with $c_{ion}^2 = 0.638(242)$. Comparing this result with the previously attained value using the hyperfine structure parameter a reveals that due to the large error of the ionic spin-orbit coupling parameter $a_{3d}^{10}(Ti^+)$ a larger uncertainty of c_{ion} follows. Our simple FA method is in good agreement with the value derived from Namiki *et al.* [95] with $c_{ion}^2 = 0.623(6)$. Namiki *et al.* evaluate the relative vibronic intensities of different optical transitions from their TiO measurements and determine the orbital characters via the electronic transition moment of TiO. They underestimate the uncertainties by taking only the molecular parameters with their uncertainties into account. It seems that the work by Namiki *et al.* makes no use of the error for their derived atomic or ionic parameters within the FAC method[94]. In following part we want to calculate the σ character of TiO by making use of our ionic value $c_{ion}^2 = 0.661(91)$ derived from the fine-structure constant A .

The molecular Fermi-contact parameter b_F is composed of the nuclear spin-electron spin interaction parameter b and the dipolar parameter c ,

$$b_F = b + c/3. \quad (\text{A.22})$$

The Fermi-contact interaction is very sensitive to the s -character of the unpaired electron. All unpaired electrons have an unquenched orbital angular momentum. Especially, the spin polarization induced by the exchange energy between unpaired and σ -bonding electrons gives a small and negative b_F contribution.

However, the Fermi interaction of non s -orbitals is expected to cancel out each other and thus to vanish.

$$b_F = 2g_S\mu_B g_N\mu_N \frac{\mu_0}{3} \frac{1}{\Sigma} \langle \Lambda\Sigma | \sum_i \hat{s}_{zi} \delta(r) | \Lambda\Sigma \rangle \quad (\text{A.23})$$

$$b_F = 1/2 (b_F(9\sigma) + b_F(1\delta)) \quad (\text{A.24})$$

$$b_F(9\sigma) = c_{4s}^{9\sigma^2} \overbrace{\left(c_{atom}^2 \underbrace{b_{F,4s}(Ti)}_{a_{4s}^{10}(Ti)} + c_{ion}^2 \underbrace{b_{F,4s}(Ti^+)}_{a_{4s}^{10}(Ti^+)} \right)}^{a_{4s}^{10}(TiO)} + c_{3d\sigma}^{9\sigma^2} a_{3d}^{10}(TiO) + c_{4p\sigma}^{9\sigma^2} a_{4p}^{10}(TiO) \quad (\text{A.25})$$

$$b_F(1\delta) = a_{3d}^{10}(TiO) \quad (\text{A.26})$$

$$\rightarrow 2b_F = c_{4s}^{9\sigma^2} a_{4s}^{10}(TiO) + \left(1 + c_{3d\sigma}^{9\sigma^2}\right) a_{3d}^{10}(TiO) + c_{4p\sigma}^{9\sigma^2} a_{4p}^{10}(TiO) \quad (\text{A.27})$$

Presuming the σ character is purely originated by the $|4s\rangle$ orbital, we simply assume that the atomic σ orbitals compensate each other,

$$2b_F - a_{3d}^{10}(TiO) = c_{4s}^{9\sigma^2} a_{4s}^{10}(TiO) \quad (\text{A.28})$$

$$\rightarrow c_{4s}^{9\sigma^2} = 0.753(35). \quad (\text{A.29})$$

By comparing our $4s$ - σ character with the previously derived value of 0.801(2) by Namiki *et al.* [95] it can be seen that it is in good agreement. Our purely experimentally derived value can be interpreted as a lower limit, because our compensation assumption of $4p_\sigma$ and $3d_\sigma$ electrons neglects further influence on the $4s$ state. By considering this large σ -character on the $4s$ orbital we assume that the remaining σ -contribution is distributed equally over the atomic $3d$ and $4p$ orbitals. Considering the large error $err(c_{4s}^{9\sigma^2}) = 0.035$ derived from the experimental measurement, the assumption is reasonable with respect to its absolute value. Applying the normalization rule the σ character coefficients are given by

$$c_{3d\sigma}^{9\sigma^2} = c_{4p\sigma}^{9\sigma^2} = 0.12(2). \quad (\text{A.30})$$

These results lead to the same values within error limits as presented by Namiki *et al.* [95] ($c_{3d\sigma}^{9\sigma^2} = 10, c_{4p\sigma}^{9\sigma^2} = 0.11$). Now, the mixed Fermi-contact parameter $a_{4p}^{10}(TiO)$ can be determined as

$$\begin{aligned} c_{3d\sigma}^{9\sigma^2} a_{3d}^{10}(TiO) &= -c_{4p\sigma}^{9\sigma^2} a_{4p}^{10}(TiO), \\ \rightarrow a_{4p}^{10}(TiO) &= -\frac{c_{3d\sigma}^{9\sigma^2}}{c_{4p\sigma}^{9\sigma^2}} a_{3d}^{10}(TiO) = -40(9) \text{ MHz}. \end{aligned} \quad (\text{A.31})$$

To summarize, this value has been determined by the compensation approach, the equally distribution assumption and with the value of atomic $3d$ mixed parameter $a_{3d}^{10}(TiO)$. This gives us a hint how much the atomic $4p$ orbital effects the Fermi-contact parameter b_F and the σ character of the $4s$ orbital. Even in case that the compensation approach is not fully valid the $4s - \sigma$ character will change only slightly.

As a last quantity of the magnetic hyperfine molecular parameter set the dipolar Fermi-contact parameter

c is investigated with

$$c = \frac{3}{2} g_S \mu_B g_N \mu_N \frac{\mu_0}{4\pi} \frac{1}{\Sigma} \langle \Lambda \Sigma | \sum_i \frac{(\cos^2 \theta_i - 1)}{r^3} \hat{s}_z | \Lambda \Sigma \rangle. \quad (\text{A.32})$$

$$c = 1/2 (c(9\sigma) + c(1\delta)) \quad (\text{A.33})$$

$$c(9\sigma) = \frac{3}{2} \left(c_{4s}^{9\sigma^2} \underbrace{\langle \cos^2 \theta - 1 \rangle_{4s}}_{=0} \overbrace{\left(c_{atom}^2 \underbrace{c_{4s}(Ti)}_{a_{4s}^{12}(Ti)} + c_{ion}^2 \underbrace{c_{4s}(Ti^+)}_{a_{4s}^{12}(Ti^+)} \right)}^{a_{4s}^{12}(TiO)} \right. \\ \left. + c_{3d\sigma}^{9\sigma^2} \underbrace{\langle \cos^2 \theta - 1 \rangle_{3d\sigma}}_{=4/7} a_{3d}^{12}(TiO) + c_{4p\sigma}^{9\sigma^2} \underbrace{\langle \cos^2 \theta - 1 \rangle_{4p\sigma}}_{=4/5} a_{4p}^{12}(TiO) \right) \quad (\text{A.34})$$

$$c(1\delta) = \frac{3}{2} \underbrace{\langle \cos^2 \theta - 1 \rangle_{3d\delta}}_{=-4/7} a_{3d}^{12}(TiO) \quad (\text{A.35})$$

$$\rightarrow 2c = \underbrace{\frac{6}{7} (c_{3d\sigma}^{9\sigma^2} - 1) a_{3d}^{12}(TiO)}_{2\mathcal{T}(a_{3d}^{12}(TiO)) \approx 33.6(27) \text{ MHz}} + \underbrace{\frac{6}{5} c_{4p\sigma}^{9\sigma^2} a_{4p}^{12}(TiO)}_{2\mathcal{T}(a_{4p}^{12}(TiO)) \approx 23.2(27) \text{ MHz}} \quad (\text{A.36})$$

$$\rightarrow a_{4p}^{12}(TiO) = 157(29) \text{ MHz}. \quad (\text{A.37})$$

The resulting mixed $4p$ atomic dipolar parameter value $a_{4p}^{12}(TiO)$ is more than three times larger than the $3d$ value $a_{3d}^{12}(TiO)$ and of opposite sign. However, with increasing σ character of the $4s$ state and the σ -compensation approach, the values of $c_{3d\sigma}^{9\sigma^2}$ and $c_{4p\sigma}^{9\sigma^2}$ decrease, therefore the $a_{4p}^{12}(TiO)$ value will also increase. The analysis on the molecular dipolar parameter c reveals that the δ orbital contribution $\mathcal{T}(a_{3d}^{12}(TiO))$ is roughly half the value derived from the $4\pi_\sigma$ orbital of TiO $\mathcal{T}(a_{4p}^{12}(TiO))$. Therefore, we may conclude that the strong polarization of TiO leads to an increase of molecular dipolar parameter c .